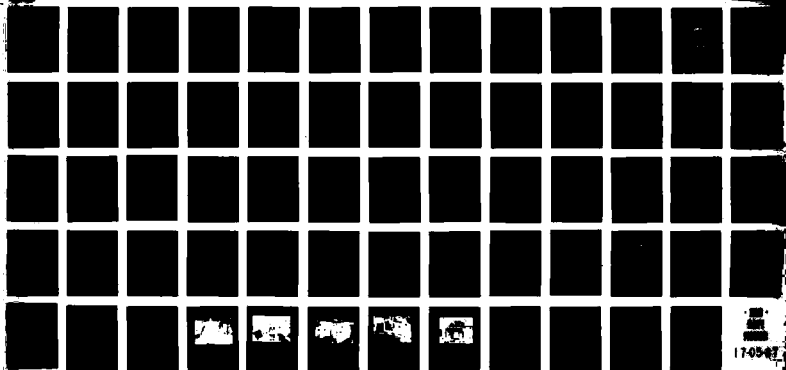


DESIGN OF AN OPTIMALLY INTEGRATED PRIMARY LAND ARCTIC  
SYSTEM (PLANS). VOLUME I: SYSTEM DESIGN. SEP 86. DEFENCE  
CLASS. ESTABLISHMENT OTTAWA, OTTAWA ONT (CAN). DREQ-946. PROJ. 8410  
UNLTD. J.C. MCMILLAN. 80 P. & 18 refs. **ADA 188730**

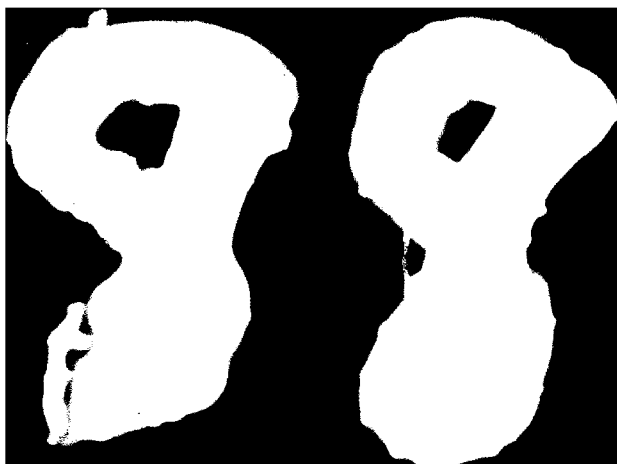
800  
188  
700

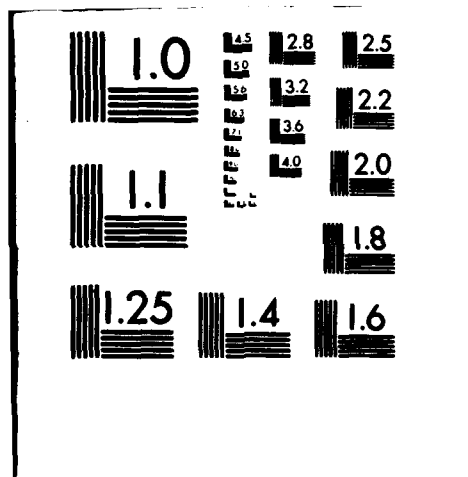
1 of 1

87-00938



174947







National  
Defence

Défense  
nationale



# **DESIGN OF AN OPTIMALLY INTEGRATED PRIMARY LAND ARCTIC NAVIGATION SYSTEM (PLANS)**

## **VOLUME I SYSTEM DESIGN**

by

J.C. McMillan

**DEFENCE RESEARCH ESTABLISHMENT OTTAWA  
REPORT NO. 948**

**Canada**

**September 1986  
Ottawa**



National  
Defence

Défense  
nationale

# **DESIGN OF AN OPTIMALLY INTEGRATED PRIMARY LAND ARCTIC NAVIGATION SYSTEM (PLANS)**

## **VOLUME I SYSTEM DESIGN**

by

**J.C. McMillan**  
*Electromagnetics Section*  
*Electronics Division*

**DEFENCE RESEARCH ESTABLISHMENT OTTAWA**  
**REPORT NO. 946**

**PCN  
041LJ**

**September 1986  
Ottawa**

## ABSTRACT

This land navigation system is designed around a dual mode gyrocompass/directional gyro, and the vehicle's odometer, with occasional Transit position fixes. A baroaltimeter is used to provide height above ellipsoid needed by the Transit receiver, and a coarse digital elevation map is used to bound the error in the barometric height. An inexpensive magnetic flux valve is used, in conjunction with a geomagnetic field model, to augment the gyro and provide a rough initial heading. An eight state extended Kalman Filter was designed to process the measurements from these sensors and thus provide an optimal estimate of the vehicles position, velocity and bearing.

Perhaps the most significant new aspect of this design is its ability to correct for the otherwise unbounded heading errors that are typical of directional gyro operation at high latitudes, where gyrocompassing is not possible and near the magnetic pole, where magnetic compasses are useless. In this design a heading correction is automatically performed whenever a Transit position fix is received while the vehicle is underway (about once every hour at high latitudes). This unique capability is due to a detailed deterministic error model, developed at DREO, which relates the error in the velocity fed into the Transit receiver during a satellite pass, to the error in the position fix that this pass yields.

## RÉSUMÉ

Ce système de navigation terrestre fait appel à un gyrocompas/gyro directionnel et à l'odomètre du véhicule, ainsi qu'à des repères occasionnels de position Transit. Un altimètre barométrique sert à déterminer la hauteur au-dessus de l'ellipsoïde, donnée nécessaire au récepteur Transit, et une carte grossière d'élévation numérique, à borner l'erreur de la hauteur barométrique. Une sonde magnétique bon marché permet, par recours à un modèle du champ géomagnétique, de compléter le gyro et d'obtenir un cap initial approximatif. Un filtre de Kalman à huit états de capacité accrue, conçu pour traiter les mesures des capteurs, fournit une estimation optimale de la position, de la vitesse et du relèvement du véhicule.

L'aspect le plus nouveau de ce système est sans doute son aptitude à corriger les erreurs de cap non bornées qui sont caractéristiques du fonctionnement des gyros directionnels à latitudes élevées, là où l'emploi du gyrocompas est impossible, ainsi que près du pôle magnétique où le compas magnétique n'a plus aucune utilité. Dans le système, il y a correction automatique du cap chaque fois qu'un repère Transit est reçu (environ une fois l'heure aux latitudes élevées), à grâce à l'exploitation d'un modèle d'erreur déterministique détaillé, mis au point par le CRDO, qui associe l'erreur de la vitesse transmise au récepteur Transit pendant un passage du satellite à l'erreur du repère fourni au cours du même passage.

## TABLE OF CONTENTS

	PAGE
ABSTRACT/RESUME .....	ii
1.0 INTRODUCTION AND PROBLEM STATEMENT.....	1
2.0 SYSTEM DESIGN .....	3
3.0 SENSOR SUBSYSTEMS .....	7
3.1.0 DEAD RECKONING .....	7
3.1.1 DR ERRORS .....	9
3.2.0 MAGNETIC HEADING .....	12
3.2.1 MAGNETIC ERRORS .....	14
3.2.2 MAGNETIC CALIBRATION .....	19
3.3.0 VERTICAL POSITIONING .....	23
3.3.1 VERTICAL ERRORS.....	25
3.4.0 TRANSIT POSITIONING.....	26
3.4.1 TRANSIT ERRORS.....	28
3.5.0 GPS POSITIONING.....	35
3.5.1 GPS ERRORS.....	37
4.0 COMPUTER.....	38
5.0 DISPLAYS .....	40
6.0 KALMAN FILTER DESIGN .....	43
6.1 STATE VECTOR .....	43
6.2 TRANSITION MATRIX .....	44
6.3 MEASUREMENT VECTOR .....	47
6.4 MEASUREMENT MATRIX .....	48
6.5 SPECIAL MEASURES .....	51
7.0 SIMULATION RESULTS .....	52

(v)

PRECEDING PAGE BLANK

PRECEDING PAGE BLANK

7.1 GYROCOMPASS MODE.....	53
7.2 DIRECTIONAL GYRO MODE .....	54
8.0 SUMMARY .....	63
REFERENCES .....	70

Volume II: TECHNICAL APPENDICES  
(RESTRICTED, UNDER SEPARATE COVER)

APPENDIX A: TERRAIN ELEVATION MAP

APPENDIX B: HORIZONTAL GEOMAGNETIC FIELD STRENGTH

APPENDIX C: ERROR STATE MODEL PARAMETER VALUES

APPENDIX D: MEASUREMENT MODEL PARAMETER VALUES

APPENDIX E: CLOSING THE LOOP IN THE TRANSIT FILTER

## TABLE OF FIGURES

	PAGE
Fig. 1. PLANS Block Diagram .....	3
2. Problem Areas for Magnetic Heading and Gyrocompass Heading ....	5
3. Magnetic Declination in the Canadian Arctic .....	13
4. Mean Hourly Range in the Geomagnetic Field .....	17
5. Magnetic Calibration Curve .....	20
6. After "Hard Iron" Calibration .....	21
7. After Full Calibration .....	22
8. Transit Position Fix Principle .....	27
9. Typical Mean Time Between Transit Fixes .....	29
10. Tropospheric Refraction Error .....	31
11. Transit Position Error due to North Input Velocity Error .....	33
12. Transit Position Error due to East Input Velocity Error .....	34
13. Transit Position Error due to Input Height Error .....	36
14. PLANS Processor Configuration .....	39
15. Main Display .....	41
16. Remote Display .....	42
17. Simulation PLANS Position Error and Covariance .....	55
18. Simulation Transit-DR Position Error .....	56
19. Simulation DR Position Error .....	57
20. Simulation PLANS Heading Error and Covariance .....	58
21. Simulation PLANS Position Error and Covariance .....	59
22. Simulation Transit-DR Position Error .....	60
23. Simulation DR Position Error .....	61
24. Simulation PLANS Heading Error and Covariance .....	62

25. External View of 1984 Installation .....	65
26. Internal View of 1984 Installation .....	66
27. External View of 1986 Installation .....	67
28. Internal View of 1986 Installation .....	68
29. PLANS Central Unit, 1986 .....	69

## 1.0 INTRODUCTION AND PROBLEM STATEMENT

In 1981, following a series of northern exercises, Mobile Command stated the requirement for a Primary Land Arctic Navigation System. The serious consequences of being lost in the arctic make accurate and reliable navigation a vital necessity. PLANS was therefore tasked by DLAEEM and is being developed at DREO to meet the arctic land navigation requirements of the Canadian Forces.

In 1982 DLAEEM tasked DREO (Reference (1)) to investigate possible methods for Primary Land Arctic Navigation. In August 1982 DREO submitted a report to DLAEEM (Reference (2)) outlining several possible navigation system options. DLAEEM selected one of the proposed system outlines and in November 1982 initiated project tasking (Reference (3)) for the Development of a Primary Land Arctic Navigation System (PLANS), based on the chosen outline.

Motivation for this study was provided by the requirement of the Canadian Forces for arctic land navigation of APCs (Armoured Personnel Carriers) which are tracked vehicles. Several significant factors combine to make the Canadian arctic a particularly difficult area in which to navigate. Firstly, there are frequent and extended periods of very low visibility, making it impossible to rely on astronomic observations or landmarks to obtain a bearing or position. Most of the north is featureless in any case, with no permanent landmarks at all. Magnetic compasses, so simple and economical for general land navigation, are quite useless over a large portion of the Canadian arctic because of the central location of the north magnetic pole. Not only is the horizontal component of the earth's magnetic field very weak in this region, but it is also highly variable in its orientation, being subject to unpredictable disturbances. Even gyrocompass operation becomes more difficult at high latitudes and eventually becomes impossible as one approaches the earth's axis of rotation, above 75 or 80 degrees latitude. These factors combine to make dead reckoning a difficult problem and, in particular, to make it almost impossible to obtain a reliable bearing using conventional methods.

Of course the usual radio navigation systems do not extend coverage into the far north, with the exception of Omega, which does not provide complete coverage in the spring and summer (see Reference (4) TASC report to ONSOU), and is not a very accurate system even under the best of conditions, providing only about 4 km. position accuracy (CEP). Omega's noise characteristics also make it unsuitable for velocity estimation, hence yielding no useful heading information.

The Transit satellite system can provide relatively good position fixes, with about 100 metre accuracy (CEP), but it is not continuous, providing a position and time fix only every 30 to 50 minutes at high latitudes, and less frequently at lower latitudes. This is not frequent enough to provide useful heading or track information, so that obtaining a bearing is still the major obstacle to high latitude navigation.

Because of these severe restrictions, northern units have been forced to make do with unwieldy astro compasses, visual terrain following, or Inuit guides none of which provide the necessary accuracy or all weather capability.

These difficulties severely restrict mobility in the arctic, where finding a fuel dump could easily be a matter of life and death. We do not presently have the capability to navigate in all weather, or while the vehicle is closed down, or in some cases even while the vehicle is moving.

Navstar GPS is another satellite navigation system which will provide the necessary coverage in the future, but this system is not expected to be fully implemented until 1987 at the earliest. At that time GPS will be far superior to Transit in both accuracy and coverage, providing continuous three dimensional position, velocity and time measurements. At the time of this study GPS was not available leaving Transit as the best choice.

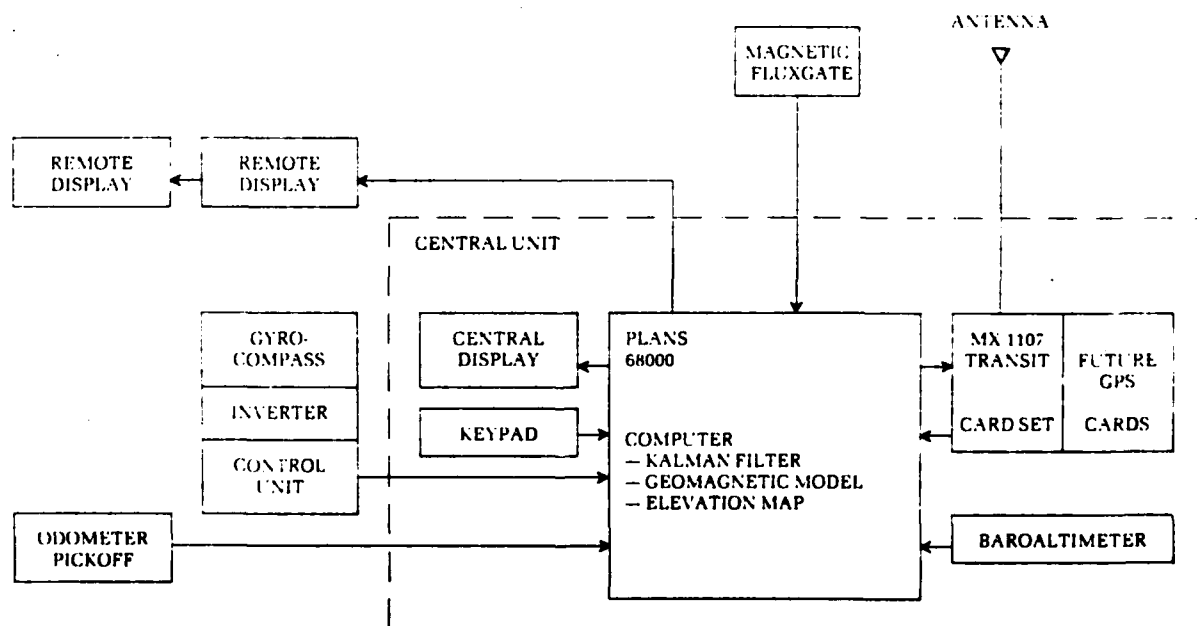
In anticipation, of GPS, however, we have selected an MX1107 Transit receiver from Magnavox that will soon have the option of being upgraded to a GPS-Transit receiver simply by changing a few boards and adding an antenna. This should be possible even before the GPS is fully operational, so that full advantage can be taken of the partial coverage that will exist. Today, for example, the few GPS satellites in orbit provide several hours per day of very accurate position and velocity information which would be of significant benefit to PLANS.

## 2.0 SYSTEM DESIGN

To overcome these severe difficulties of navigation in the Canadian Arctic an optimally integrated system approach has been taken, using a mix of self contained sensors with a satellite receiver.

The basic system design of PLANS is as shown in Figure 1. The heart of the system is a Motorola 68000, a powerful 16-bit microprocessor, programmed with sophisticated optimal integration software, developed at DREO, to filter the sensor output and perform the navigation tasks. This software also includes some special routines to apply corrections to some of the sensor measurements, perform sensor calibration functions, perform waypoint calculations and drive the various displays.

Figure 1. PLANS BLOCK DIAGRAM



The central unit, shown by the dashed line, is about 2 cubic feet in size in our laboratory model and contains the microprocessor, a liquid crystal central display, a keypad, a repackaged MX1107 Transit receiver, a baroaltimeter and all necessary power supplies and sensor interfaces.



External to this central unit, but inside the vehicle, is a dual mode gyrocompass/directional gyro, two remote liquid crystal displays (for the driver and the commander) and a pickoff from the vehicle odometer. On the vehicle roof is mounted a magnetic flux valve and the Transit antenna.

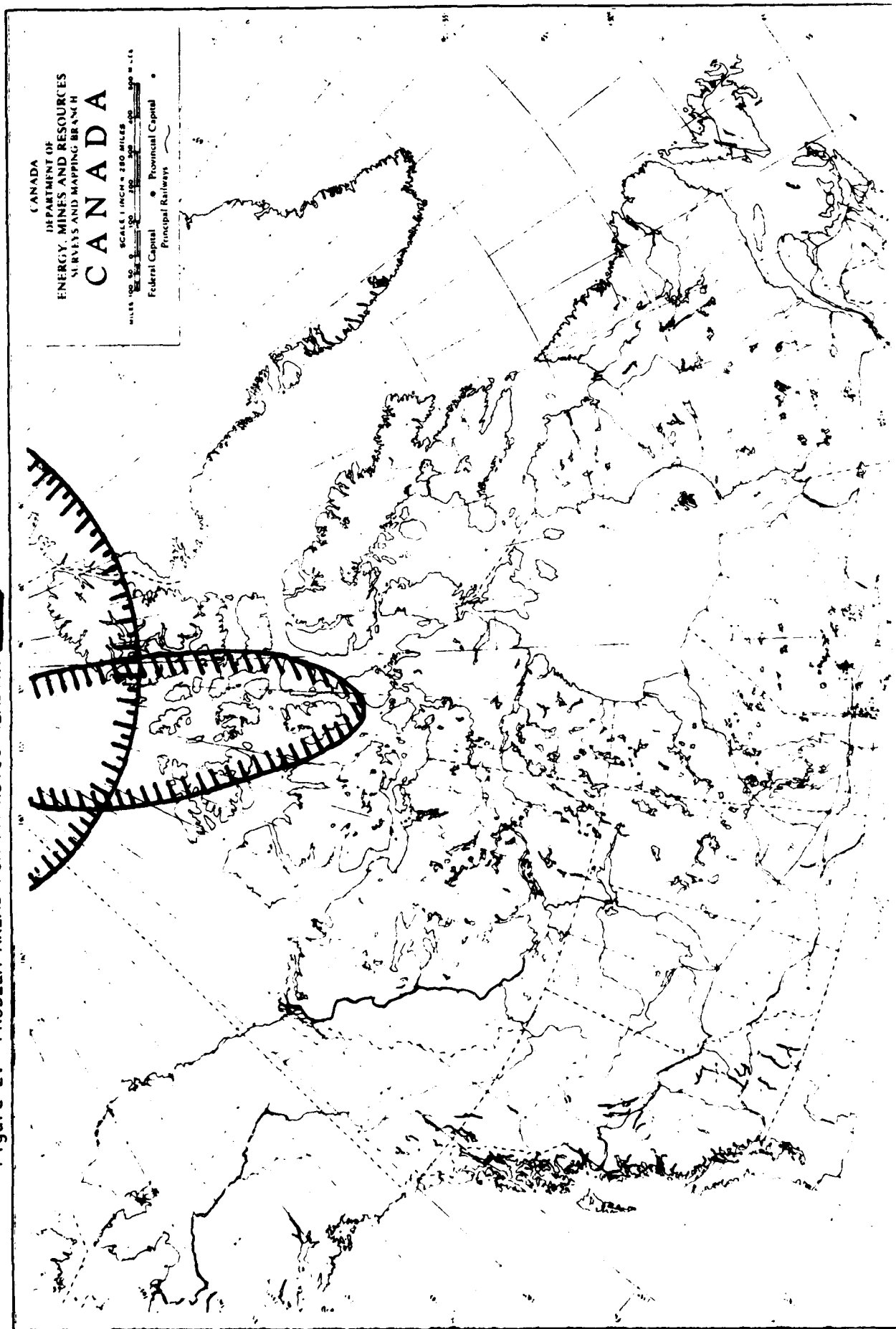
The primary navigation subsystem is a dead reckoning system composed of a dual mode gyrocompass/directional gyro which is used as the primary directional sensor, along with the vehicle odometer to measure speed (or distance made good). Dead reckoning position errors of course will increase with time in an unbounded manner. This DR error growth will be particularly serious at extreme latitudes where the gyrocompass must operate in directional gyro mode and the heading error itself will increase in time.

At extreme latitudes, north of about 80 degrees, there is not enough distance from the earth's rotational axis to support gyrocompassing. In this situation the gyro will have to be used in directional gyro (DG) mode at which time its heading will slowly drift in an unbounded manner and it will not be able to provide an initial heading. Therefore the inexpensive magnetic flux valve is used to supply an approximate initial heading, as well as to bound this DG heading error. This of course requires a detailed geomagnetic model (see Reference (5), NOAA GEOMAG IGRF80A), implemented on the microprocessor, to provide the substantial magnetic declination that exists in the Canadian arctic, and to provide the filter with estimates of the uncertainty in this magnetic declination, which is also quite significant over a large portion of this area (see Ref. (6), Witham, Loomer and Niblett, 1960).

Even at lower latitudes, where gyrocompassing is possible, the flux valve will be useful to the Kalman filter because the error characteristics of the flux valve heading are very different from those of the gyro. This flux valve will also be useful for detecting error conditions in the gyro, for bounding dynamically induced gyro errors, and for providing a secondary backup for the important heading measurement. Of course there are areas where even a flux valve will be unable to produce a useful bearing, but the geomagnetic model can predict this and inform the filter to deweight these measurements.

Figure 2 illustrates the regions where gyrocompassing will be impossible (with the Arma Brown gyro) and where the magnetic heading will be unusable. These regions of course are not as sharply delineated as the figure shows, so there is a small region of possible overlap where neither gyrocompass nor flux valve will be reliable.

Figure 2. PROBLEM AREAS FOR MAGNETIC HEADING  AND GYROCOMPASS HEADING 



It was originally intended to solve this heading problem by using the Transit signal, with two antennae in an interferometry configuration, to obtain another heading measurement. A feasibility study was commissioned to study this technique, known as Aztrans (AZimuth from TRANSit) and the initial results looked very promising. EDO Canada (formerly JMR Instruments Ltd.), the only Canadian manufacturer of Transit receivers, was contracted to conduct this study, and their Phase I Report was very positive, predicting accuracy of about 0.5 degrees (see Reference (7), July 1983). After a Phase II contract had been negotiated (July 1984) to build a working Aztrans receiver, EDO decided that the technical risk was too great and that they did not wish to continue. There was some serious concern about multipath problems on the APC adversely affecting the Transit signal reception. It was also anticipated that there would be some difficulty with the RF design required to add the third 400 MHz channel to the JMR 2000.

However another method has been developed at DREO to obtain heading information from the Transit position fixes without having to modify the receiver in any way. This new method employs a detailed error model (see Reference (8)) which allows the Kalman Filter, described below, to extract a velocity correction (ie. heading and speed corrections) from a Transit position fix that was taken while the vehicle was underway. This allows us to use an off-the-shelf dual channel Transit receiver. We chose the Magnavox 1107 for this. One advantage of the MX1107 is that Magnavox is developing a GPS receiver card set and a GPS-Transit antenna that will allow this receiver to be easily upgraded to a GPS-Transit receiver simply by changing a few cards and adding another antenna.

This Transit receiver naturally requires that velocity and height above geoid be constantly supplied. Any error in these supplied quantities will introduce a proportional error into the position fixes that the receiver produces. Since the DR velocity is expected to have substantial errors, as will be described below, it was decided to feed the Kalman filters velocity estimate into the Transit receiver. To supply the height above geoid a baroaltimeter is used, along with a coarse digital map created at DREO. The Kalman filter uses both the barometric measurements and the map, along with error models of both, to form an optimal estimate of height above geoid. It is this filtered estimate that is supplied to the Transit receiver.

In the next chapter we shall examine these subsystems in more detail.

### 3.0 SENSOR SUBSYSTEMS

#### 3.1.0 DEAD RECKONING

Dead reckoning (DR) is the determination of the position at time  $T+dT$  by knowing the initial position at time  $T$  and integrating the velocity vector from  $T$  to  $T+dT$ . For land and sea navigation the horizontal velocity vector is generally obtained by measuring the heading and speed. For PLANS the heading is measured using a dual mode gyro and the speed is measured using the vehicle odometer.

To obtain this speed measurement a Masstech TR10 "Yellow Jacket" was installed on the odometer cable. This odometer cable is mechanically linked to the drive train of the APC, and rotates at a rate proportional to the drive shaft rate which is nominally proportional to the vehicle speed over the ground. The speed sensor (yellow jacket) is a magnetically actuated reed SPST switch, which closes 8 times per revolution with a 60% duty cycle. This then generates 8 pulses per revolution, which can be used to measure the along-track distance travelled by the vehicle. These pulses are fed directly to the PLANS computer which counts the pulses over the integrating interval which, for PLANS, is .25 seconds as measured by the computer's onboard clock. This pulse count  $C$  is then multiplied by the appropriate scale factor  $F$ , to obtain the distance  $D$ , moved over the ground during the time interval  $dT$ . The vehicles average speed over this interval is therefore  $D/dT = C F/dT$ .

The gyrocompass measurement is assumed to be the clockwise angle from true north to the horizontal velocity vector. The north and east dead reckoning velocity components are therefore:

$$V_n = \frac{C * F * \cos \theta}{dT} \quad (1)$$

$$V_e = \frac{C * F * \sin \theta}{dT}$$

These DR velocity components are measured at a 4 Hz rate, and are integrated to provide a DR horizontal position estimate every second.

In PLANS the position is calculated and expressed as geodetic latitude and longitude, using the WGS72 ellipsoid (World Geodetic Survey 1972). The integration of velocity is therefore done as follows:

$$\begin{aligned} \text{LAT} (T + dT) &= \text{LAT}(T) + V_n * dT / (R_n + h) \\ \text{LON} (T + dT) &= \text{LON}(T) + V_e * dT / \cos(\text{LAT}) * (R_e + h) \end{aligned} \quad (2)$$

where h is the height of the vehicle above the ellipsoid, and  $R_n$  and  $R_e$  are the meridional (north-south) and prime (east-west) radii of curvature of the ellipsoid:

$$\begin{aligned} R_n &= \frac{A^2}{B(1 + E \cos^2 (\text{LAT}))^{3/2}} \\ R_e &= \frac{A^2}{B(1 + E \cos^2 (\text{LAT}))^{1/2}} \end{aligned} \quad (3)$$

where

$$E = A^2/B^2 - 1.$$

and A and B are the semimajor and semiminor axes of the ellipsoid. We have chosen the WGS72 ellipsoid because it is the modern standard and is used by the Transit and GPS satellite systems. Although this will likely be replaced by WGS84 when the GPS satellite system becomes operational, the difference between these two systems is negligible. PLANS can also display the position in UTM coordinates (Universal Transverse Mercator) in the form of Northings and Eastings, to comply with military charts. It should be mentioned however, that these UTM coordinates are not particularly well suited to high latitude navigation, where the "grid" becomes highly distorted. Reference (9) gives more detail.

Of course equation (1) assumes that the vehicle is moving in the local horizontal plane, in the direction indicated by the gyro heading, at the speed indicated by the odometer. If a reliable pitch angle is available, the terms in equation (1) should be multiplied by the cosine of this pitch angle, to give the correct horizontal components of the velocity. The errors in this DR system are discussed in the next section.

The dual mode gyro initially chosen was an Arma-Brown MK V (Mod 4) which is a "small" and rugged gyrocompass, designed for land navigation, with accuracy specified to be better than 1 degree in gyrocompass mode and 2 degrees per hour in directional gyro mode. It also claims to be capable of gyrocompassing at latitudes as high as 80 degrees. This gyro requires its own external inverter and control unit, making the heading subsystem about 40,000 cc in volume (1.5 cubic feet) and about 32 kilograms in weight. This gyro is unheated and draws about 150 watts during regular operation.

This Arma-Brown gyro was ordered in December 1982, and received in March of 1983. Due to faulty wiring it had to be returned for repairs, which were performed in Montreal. We received the repaired gyro in the fall of 1983, at which time static tests were conducted at DREO. It was then discovered that the gyro would have to be heated. Low temperature testing revealed that the gyro would not operate at all if its temperature was below -10 degrees centigrade and that it took 2.5 hours

to settle at +8 degrees centigrade. Even at room temperature the gyro required 45 minutes to settle, after careful leveling and from an initial heading of only +/-2 degrees off true. As a consequence of our careful testing, the manufacturer redefined the gyro specifications and provided us, free of charge, with a band heater. This band heater draws an additional 175 watts of power, and is to be used for about 30 minutes during gyro startup. Needless to say, this is a serious disadvantage.

Some limited dynamic gyro tests were conducted in an APC (provided by DLAEEM) in November and December of 1983. Using a theodolite as reference, it was determined that the accuracy of the Arma-Brown gyro, in gyrocompass mode, after settling, was in the order of 1 degree, as claimed by the manufacturer. More detailed dynamic testing was performed after the complete PLANS system was assembled in the autumn of 1984, as described in chapter 7.0 below.

Because of the large size, weight and power consumption of the Arma-Brown system, it is intended that it be replaced as soon as a better sensor is identified. For this purpose a preproduction model of a Lear-Siegler strapdown vehicle Reference Unit (S/D VRU) model 910B (which should be in production by early 1986) has been purchased. This unit occupies about 4,700 cc in volume, weighs only about 4.5 kg, and consumes about 60 watts of power. Another possible advantage of this unit is that it provides attitude information as well. Lear Siegler claims 1 degree alignment accuracy, but it does not gyrocompass dynamically (the vehicle must be stationary) as the Arma-Brown system does, making general accuracy comparison difficult. The initial alignment gyrocompassing however is very fast, requiring less than 5 minutes, compared to the 30 plus minutes required by the Arma Brown. Unfortunately however, the Lear Siegler does not have a coarse align capability, and therefore it will not align properly unless the vehicle's heading is within about 20 degrees of north, and it also requires continuous speed input.

### 3.1.1 DR ERRORS

There are many possible sources of error in this DR calculation, most of which can be categorized as speed or track errors. The important errors are as follows:

"Speed" errors:

- s1 - vehicle track slippage (along track)
- s2 - odometer scale factor error
- s3 - computer clock error
- s4 - non-horizontal component of velocity
- s5 - sensor fault
- s6 - data communication fault
- s7 - invalidation of odometer when vehicle is used in amphibious mode, or on drifting ice.

Track errors:

- t1 - gyro misalignment (not exactly along vehicle axis)
- t2 - gyrocompassing error (if latitude is below about 80 deg.)
- t3 - directional gyro error (if latitude is above about 80 deg.)
- t4 - vehicle lateral track slippage (crabbing)
- t5 - discretization error (resolution)
- t6 - data communication fault
- t7 - invalidation of heading as track when in amphibious mode, or on drifting ice.

Of all the above DR error sources we expect the most significant to be s1, s2, t1 and t3. Although other errors such as s7 and t7 are potentially more serious, they are much less likely to occur.

For non-zero pitch angles, the error incurred by neglecting the non-horizontal component of the velocity, called s4 here, is a scale factor equal to  $(1 - \cos(\text{pitch}))$ . This is an error of less than 1% of distance travelled for pitch angles of less than 8 degrees, which is a grade of about 1 to 7. At steeper grades this error increases fairly rapidly (about 4% error at 16 degrees pitch for example) but it is expected that on the average s4 will be less than 1%. The effect of this error is to slightly overestimate the speed on uneven or sloping terrain, which is similar to the effect of vehicle track slippage s1, which typically also causes a random overestimation of speed.

In September of 1983 preliminary speed sensor tests were performed at DREO on the Masstech TR10 odometer pickoff. The primary objective was to determine the scale factor F, which was found to be about .2094 metres per pulse, resulting in a resolution of .2094 metres. This was found by driving the APC back and forth across a carefully measured straight stretch of asphalt road. The details of this test are described in Reference (10). In conjunction with determining this scale factor, the repeatable accuracy of this speed sensor installation was found to be better than 1%. These test conditions were of course far from typical, and more extensive and definitive results were obtained during system tests which were conducted over a larger course with varying road surfaces, at DREO in the summers of 1984 and 1985.

In 1985 the Masstech pickoff was replaced with a pickoff that came with the new Lear Siegler gyro. This new pickoff has a higher resolution of about .0027 metres, and consequently a different scale factor, .0027 metres/pulse. This scale factor was determined by driving between two surveyed points separated by more than a kilometer.

The combination of vehicle track slippage s1, scale factor error s2, and pitch induced error s4 is expected to produce approximately 1% error in distance travelled, which is converted in PLANS to speed. Since s1 will be constant and s2 and s4 will be slowly varying, this error can be estimated by the Kalman filter, and then removed in the software (to

the extent that it can be estimated). If for example good GPS position measurements are available even briefly, then the filter could effectively calibrate the odometer and thereafter remove part of this error.

The heading error consists mainly of the static error  $t_1$  plus the dynamic error, either  $t_2$  or  $t_3$ . The static error is largely due to the difficulty of accurately aligning the gyro sensitive axis to the vehicle's forward movement axis during installation. In practice the gyro is mounted by aligning a mark on the gyro housing, representing the sensitive axis, to a mark on a mounting plate, representing the vehicle's forward axis. The difficulty in practice is accurately installing the mounting plate in each vehicle. We found that the resulting error  $t_2$  could be kept below 1 degree without much difficulty, by first doing a rough mounting, then driving from a known starting point to another surveyed point several hundred metres away (over a smooth hard surface). The deadreckoned solution at the second point will simply be rotated with respect to the known survey point by an angle equal to the misalignment. The mounting plate can then be rotated by this angle to reduce  $t_1$ .

The dynamic heading error characteristics will depend a great deal on the gyro mode of operation (gyrocompass or directional gyro), and also on the latitude when in gyrocompass mode. In gyrocompass mode the heading error  $t_2$  is expected to be slowly varying in a bounded manner, at about 1 degree (1 sigma) at low latitudes, and increasing with latitude as follows:

$$\text{mean heading error} = \frac{1 \text{ degree}}{\cos(\text{latitude})} \quad (4)$$

In directional gyro mode the heading error  $t_3$  will vary slowly in an unbounded manner, drifting at a rate of approximately 1 degree/hour (1 sigma). This drift rate will be unaffected by latitude.

The size and characteristics of the gyro errors depend to a large extent on the general design of the unit being used. For example, the Arma Brown is a pendulous gimbaled gyrocompass, whereas the Lear Siegler unit is a strap-down vertical reference unit with one dual axis tuned-rotor gyro, two level accelerometers, and a distance measurement unit (DMU), which attaches to the vehicle odometer cable. This DMU input is very important to the Lear Siegler system: because of its mechanization, it is subject to significant dynamic errors due to track slippage or to error in the DMU input.

The gyro heading error is estimated by the Kalman filter. In fact two states are devoted to estimating this error (see section 6.1); one to estimate the gyro drift rate when in DG mode, and one to estimate the heading error itself, (which is the integral of the drift rate when in DG mode). If the vehicle is not moving then the gyro drift rate can be measured directly, otherwise the necessary additional heading information comes from the magnetic sensor and to some extent from the change in Transit and GPS position measurements. As with the odometer, the filter can then estimate and partially remove the gyro heading error.

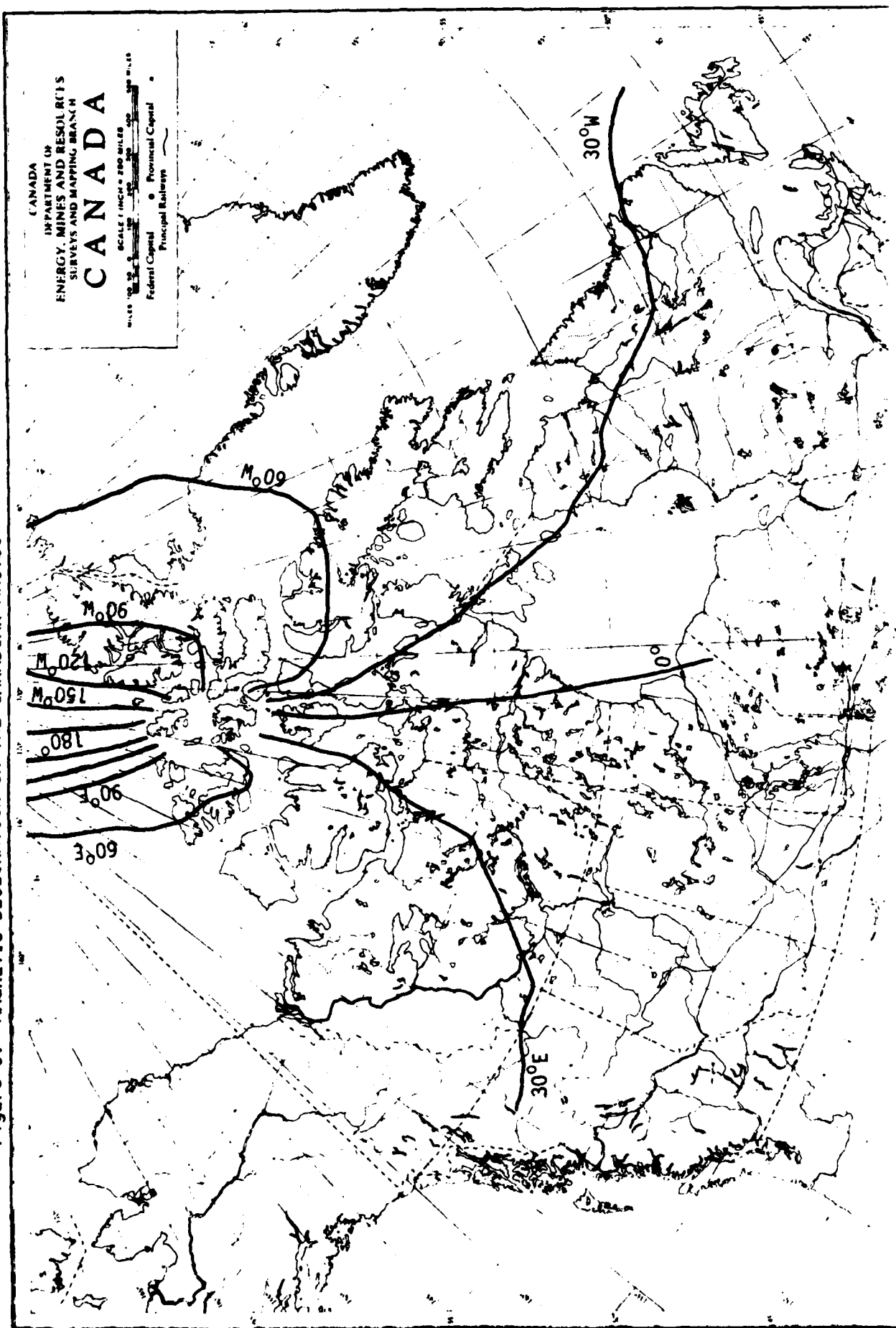
### 3.2.0 MAGNETIC HEADING

The magnetic flux valve measures the direction of maximum horizontal magnetic field strength. Since the earth's magnetic field is roughly aligned with its axis of rotation, on a global scale the north magnetic pole is close to the geographic north pole. Therefore at low latitudes the magnetic direction is approximately north. Unfortunately however, the north magnetic pole is almost centrally located in the Canadian arctic, so that the magnetic field direction differs substantially from true north throughout the Canadian arctic. The difference between true north and magnetic north is known as the Magnetic Variation, or the Magnetic Declination, and just how significant this declination can be is seen in Figure 3, which shows some lines of magnetic declination in the Canadian Arctic.

To obtain a useable magnetic heading it is therefore necessary to apply the magnetic declination correction to the measurement. This is especially important at higher latitudes where the declination is generally very large. To provide this correction we obtained detailed geomagnetic field models from the American National Oceanographic and Atmospheric Administration (NOAA). The model selected is known as IGRF80A (International Geomagnetic Reference Field 1980A), which is a global spherical harmonic model of degree and order 10 in the main field and 10 in the secular field. The program purchased from NOAA was written in Fortran for a Univac 1100. We therefore had to modify it to run on RSX and then translate it to the C language, so that it could be cross compiled to the PLANS microprocessor, a Motorola 68000.

This program actually computes much more than just the magnetic declination. It also provides the horizontal field strength, the dip angle, the total field strength and its three cartesian components as well as the rate of change of each of these quantities. The dip angle and horizontal field strength are useful in predicting the accuracy of the magnetic flux valve measurement.

Figure 3. MAGNETIC DECLINATION IN THE CANADIAN ARCTIC



For the PLANS development model we are using a Marinex Compass Sensor Unit, Type 900111, which incorporates a gimballed fluxgate sensor assembly capable of directly measuring the horizontal components of the earth's magnetic field. This sensor unit is in a single, weather-proofed container originally intended for marine applications. It contains two sensing units aligned 90 degrees apart to provide the full range of unambiguous heading by generating two output signals proportional to the sine and the cosine of the magnetic heading. It occupies a volume of only about 900 cc and consumes less than 4 watts of power. The manufacturer claims that it will provide magnetic heading accurate to 2 degrees for magnetic dip angle from 0 to 80 degrees (or horizontal field strength from 40,000 Gamma to 10,000 Gamma). Although this excludes a large portion of northern Canada, it appears that the problem there is due to an electronic scaling problem which can perhaps be overcome by software scaling. Another problem with this unit is that it is only specified down to -15°C. Since it must be mounted externally, it will likely experience much lower temperatures in the arctic. Because of these problems we are still looking for a more suitable magnetic sensor unit.

One option that we will be testing is to replace the 2-axis gimballed fluxgate sensor with a 3-axis strapped-down sensor. We have ordered a Model TAM7, 3-axis strapdown hybrid magnetometer from Dowty RFL International Inc. This unit is specified down to -33°C with no loss of performance, and down to -51°C with reduced performance. This is a more rugged and compact unit than the Marinex, but it requires an external attitude measurement in order to transform the measured magnetic field from vehicle frame to the locally horizontal frame. Although the Lear Siegler gyro can provide this attitude information, it will likely be subjected to dynamically induced errors similar to those experienced by the gimballed unit (described in more detail in the next section). Two reasons why the Lear Siegler determined attitude may be better than the pendulous gimbal determined attitude are both due to location. The Lear Siegler is inside the vehicle where it will be warmer than the Marinex gimbal, and it will also be closer to the vehicle's centre. The fluxvalve is mounted on the external rear corner of the vehicle to avoid the worst magnetic field distortions from the vehicle. Unfortunately this also maximizes the lever arm length from the vehicle centre of motion, which magnifies the non-gravitational accelerations experienced by the gimbal, which in turn causes the large gimbal attitude errors. As will be described below, these attitude errors result in magnetic heading errors.

### 3.2.1 MAGNETIC ERRORS

The error in magnetic heading is due largely to unpredictable variations in the direction of the local magnetic field, but there can also be significant sensor errors, especially if a pendulous gimbal is used to keep the sensor horizontal. The most important factors affecting magnetic heading accuracy are as follows:

- m1 - local variations in the geomagnetic field
- m2 - magnetic fields induced in the vehicle by the earth's field
- m3 - permanent fields in the vehicle
- m4 - sensor misalignment errors
- m5 - dynamically induced deviations from the horizontal (gimballed systems)
- m6 - low horizontal field strength

The most obvious source of error in magnetic heading is due to the fact that the magnetic field vector does not generally point towards the geographic north. As described in section 3.2 above, the large scale component of m1 can be modelled fairly well. On a local scale the magnetic field can be affected by permanent or induced magnetic fields in the vehicle itself or some nearby structure (manmade or geological). The permanent field of the vehicle m3, will add vectorially to the earth's magnetic field vector, introducing a heading error that varies sinusoidally as a function of the vehicle's geographic heading, with a period of 360 degrees. This is often called the "hard-iron effect", and is due to magnetized portions of the vehicle or its load. If the load effect can be neglected then this error can be compensated for by knowing its amplitude and phase. The induced field m2, known as the "soft-iron effect", is due to the high permeability portions of the vehicle warping the earth's magnetic field. This error is similar to m3 in that it can be compensated for by determining its amplitude and phase, but different in that it is a function of magnetic heading and that m2 has a period of 180 degrees.

The magnetic heading error can then be expressed as

$$\begin{aligned} \theta - \theta_m &= m1(LAT, LON, t) + m2(\theta) + m3(\theta_m) + m4 + m5(t) \\ &\approx m1(t) + a2 * \sin(2\theta_m + \delta2) + a3 * \sin(\theta + \delta3) + m4 + m5(t) \end{aligned} \quad (5)$$

where a2, a3, m4 and  $\delta2$  and  $\delta3$  are constants. If the magnetic heading  $\theta_m$  has been already adjusted using the geomagnetic field models prediction, then the remaining local variations m1(t) will seem to be randomly varying in a continuous manner, much like a first order Markov process, which is what we use to model this error. The dynamically induced error m5(t) will be largely uncorrelated, and can be treated as a random white measurement noise.

As with the gyro, the magnetic sensor is intended to measure the heading of the centre line of the vehicle, but actually measures the heading of its sensitive axis. Therefore its sensitive axis has to be properly aligned parallel to the vehicle line. The angle between the sensor axis and the vehicle centre line is the sensor misalignment error m4. Although this misalignment is presumably quite small (less than one degree), it will introduce a constant bias error into the heading measurement.

Although a good geomagnetic field model can correct for the spatially varying component of  $m_1$ , there will remain a significant time varying component, especially in the vicinity of the magnetic poles. This temporal fluctuation in the field is the most serious problem in obtaining an accurate magnetic heading, especially if it is magnified by the geometric effect near the poles where the field has a large vertical component and a small horizontal component. This near vertical alignment makes it very difficult, if not impossible, for a flux valve to obtain any heading measurement at all. This is primarily because the change in the magnetic declination, and hence in magnetic heading, as a function of temporal changes in the north and east components of the magnetic field  $dX$  and  $dY$ , is inversely proportional to the horizontal field strength  $H$ :

$$d\theta = \frac{-\sin\theta * dX + \cos\theta * dY}{H} \quad (6)$$

where  $d\theta$  is the change in the magnetic declination, in radians. Equation (6) is a purely geometric relationship, found by differentiating the definition  $\theta = \arctan (X/Y)$ .

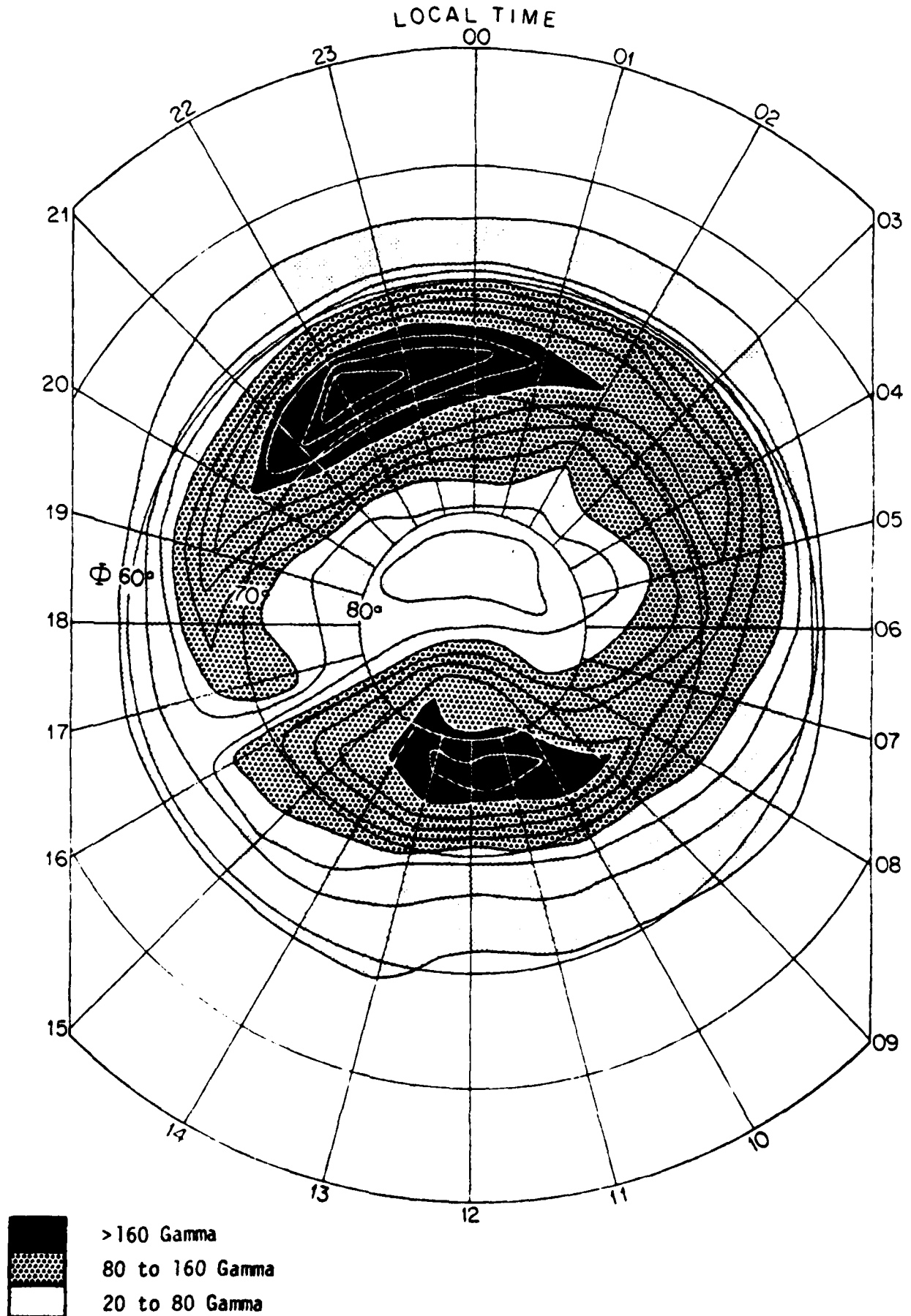
These horizontal magnetic field components  $X$  and  $Y$  exhibit substantial temporal variation, especially in the far north. Although these variations are random, their expected magnitude does vary in a fairly regular fashion with time of day and with season. There is also a correlation with the 11-year solar cycle and the 27-day period of the sun's rotation. The mean hourly variation of these field components is shown in Figure 4 for an area around the north magnetic pole (the coordinates are Geomagnetic latitude, which is centred on the magnetic pole). Over a large portion of the Canadian arctic, this average variation is typically on the order of 100 gammas, but the actual variation can at times easily be as much as 500 gammas. The horizontal field strength  $H$  is generally less than 17,000 Gammas in the Canadian Arctic, resulting in declination changes of more than 3 degrees, and in some areas more than 10 degrees (see Reference (6) for more details).

Another source of magnetic heading error  $m_5$  is also strongly affected by the horizontal field strength. This is due in part to the problem of keeping the flux valve vertically aligned. Any small misalignment will cause the strong vertical component of the field to project into the flux valve's "horizontal" plane and introduce a large unpredictable error. This is described in reference 12 as a function of an acceleration that is assumed to have caused the pendulous gimbal to tilt. For small accelerations the resulting heading error is approximated in Reference 12 (page 435) by an expression equivalent to:

$$d\theta = \frac{A*V}{g*H} \sin(\beta) \quad (7)$$

Figure 4. MEAN HOURLY RANGE IN THE GEOMAGNETIC FIELD

-17-



where V and H are the vertical and horizontal components of the geomagnetic field, A is the small acceleration, g is the gravitational acceleration and  $\beta$  is the angle between the acceleration vector and north. This is clearly sensitive to small horizontal field strength.

These dynamically induced errors were examined in more detail at DREO as a function of gimbal pitch and roll angles  $\phi$  and  $\psi$ , and magnetic field components X, Y, and Z (north, east and down). The exact expression is rather long, but for a small pitch angle  $\phi$  and zero roll, the heading error is approximately

$$d\theta = \tan^{-1} \left\{ \frac{\phi * Z * (X \sin \theta + Y \cos \theta)}{H * H - \phi * Z * (X \cos \theta - Y \sin \theta)} \right\} \quad (8)$$

where of course the horizontal field strength  $H = \sqrt{X^2 + Y^2}$ , and where the heading is  $\theta$ . Using the known field strength components for the Ottawa area, and a heading of zero degrees, this expression becomes

$$d\theta = \tan^{-1} \left\{ \frac{-\phi}{1.2843 - 3.9917 * \phi} \right\} \quad (9)$$

which has a singularity at pitch angle of only 18.4 degrees. In other words a pitch angle of only 18.4 degrees or more would completely destroy the magnetic heading measurement.

It has been our experience with our gimballed magnetic flux valve that these dynamically induced heading errors are indeed quite serious during normal operation of the host vehicle, even over rather smooth roads. At the one  $H_z$  sampling rate that we were using, this produced a heading error of several degrees that appeared largely uncorrelated in time.

The effect of this uncorrelated noise can be significantly reduced by implementing a simple pre-filter. This usually involves the averaging of several measurements, say n of them, which will reduce the noise level by a factor of  $1/\sqrt{n}$ . By increasing n the noise level can be decreased, but if the heading is changing this will also decrease the responsiveness to this change, introducing a lag. To overcome this we use as a basic measurement the difference between the gyro heading and the magnetic heading. This difference effectively removes the dynamics from the raw magnetic measurement, allowing the prefilter to remove most of the uncorrelated noise and the Kalman filter to remove most of the remaining time-correlated error.

### 3.2.2 MAGNETIC CALIBRATION

The effect of the sensor misalignment and the permanent and induced fields can be minimized by performing a magnetic calibration. This can be done by measuring both the magnetic heading and the gyrocompass heading while slowly rotating the vehicle. Since the gyrocompass errors are small compared to the magnetic errors, the difference between magnetic and gyro heading is approximately equal to the magnetic heading error, which can be tabulated as a function of the heading. This function can then be closely approximated by the sum of a constant (from  $m_1$  and  $m_4$ ), the sinusoids in equation (5) (from  $m_2$  and  $m_3$ ) and the dynamically induced errors ( $m_5$ ). The dynamically induced errors can be minimized by driving slowly over a large circle on a smooth surface to "rotate" the vehicle. Since these dynamic errors are uncorrelated, their effect can be further reduced by driving several times around the circle.

When this was done at DREO, with the compass sensor unit mounted on the top right rear corner of a command vehicle (an M577), the calibration curve was as shown figure (5), where the raw magnetic heading is shown (uncorrected for magnetic variation). The geomagnetic field model indicates that the magnetic variation in the Ottawa area is about  $13.5^\circ$ , which should be subtracted from the data of figure 5 in order that it represents the expression given by equation 5. From this it is easy to visually estimate the constant and first order sinusoid (hard iron effect) to be

$$m_4 \approx 17^\circ - 13.5^\circ = 3.5^\circ$$

$$m_3 \approx 20^\circ \sin(\theta + 20^\circ) \quad (10)$$

When these two terms are subtracted off, the remaining error is as seen in figure 6. The second order sinusoid (soft iron effect  $m_2$ ) is now clearly visible and can be estimated as

$$m_2 \approx 4^\circ \sin(2\theta - 50^\circ) \quad (11)$$

When this is also subtracted off, what remains is seen in figure 7 to be quite uncorrelated, and is due largely to gimbal errors.

Once this calibration has been done, the terms shown in equation (10) and (11) can be used to greatly improve the magnetic heading accuracy. It must be kept in mind of course that the estimate for sensor misalignment  $m_4$  will be corrupted by the local value of  $m_1$ , and that the induced field effect  $m_2$  is due to the earth's field in the calibration area, and hence will be different if the vehicle moves to an area where the earth's field is substantially different. Of course all three calibration terms will be invalid if the magnetic sensor is moved (to a different location on the vehicle, or to a different type of vehicle).

Figure 5. MAGNETIC CALIBRATION CURVE

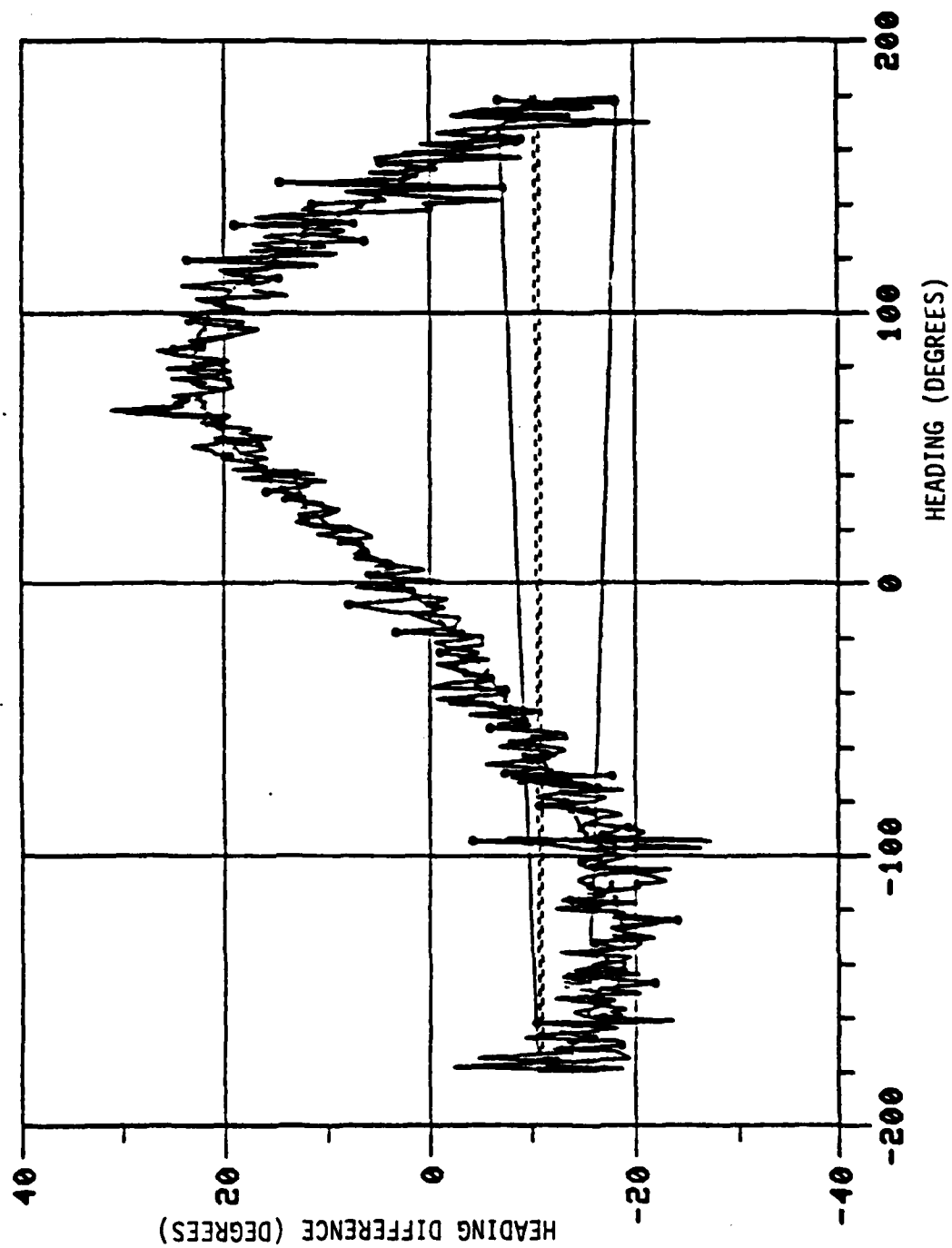


Figure 6. AFTER "HARD IRON" CALIBRATION

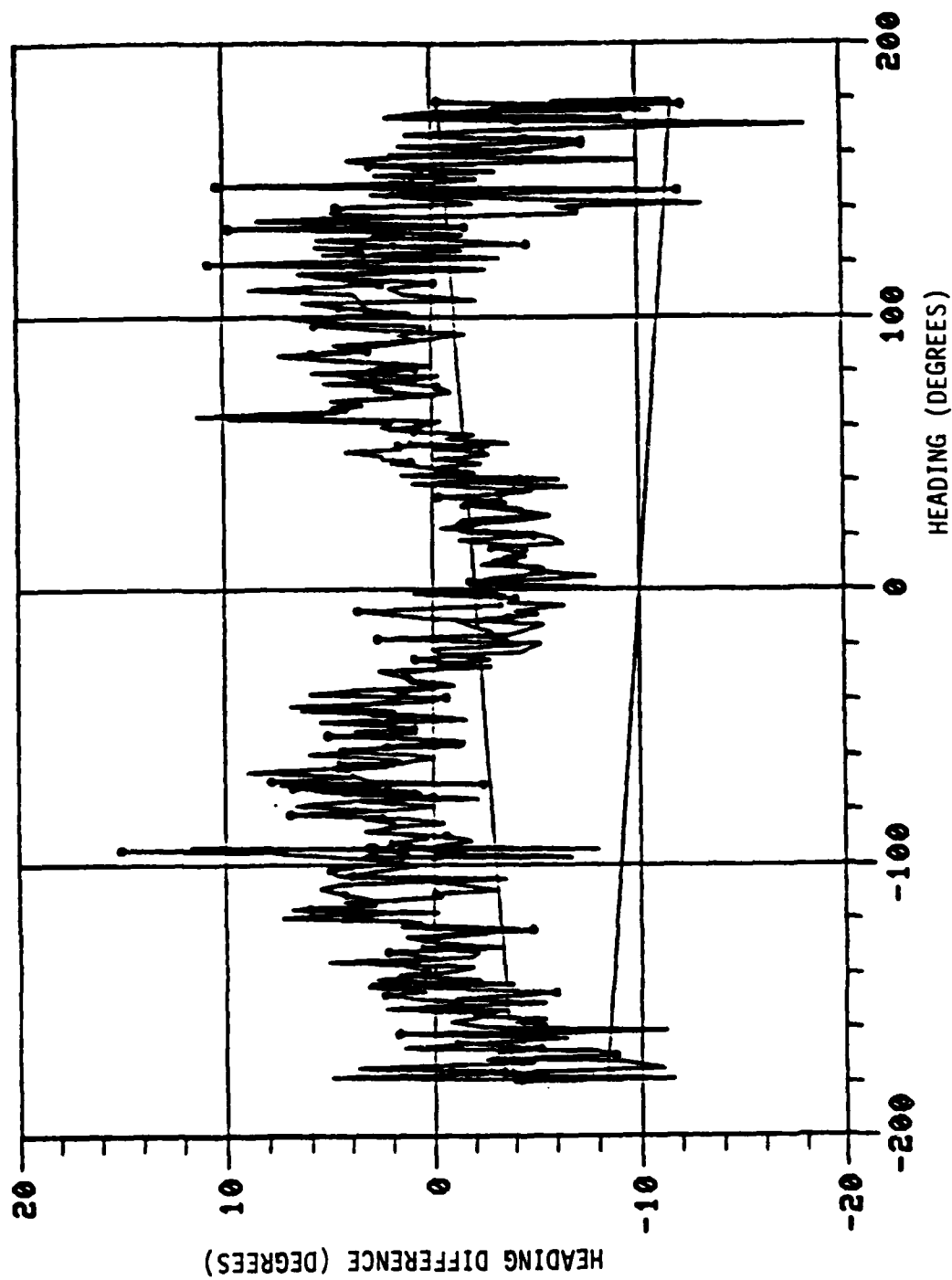
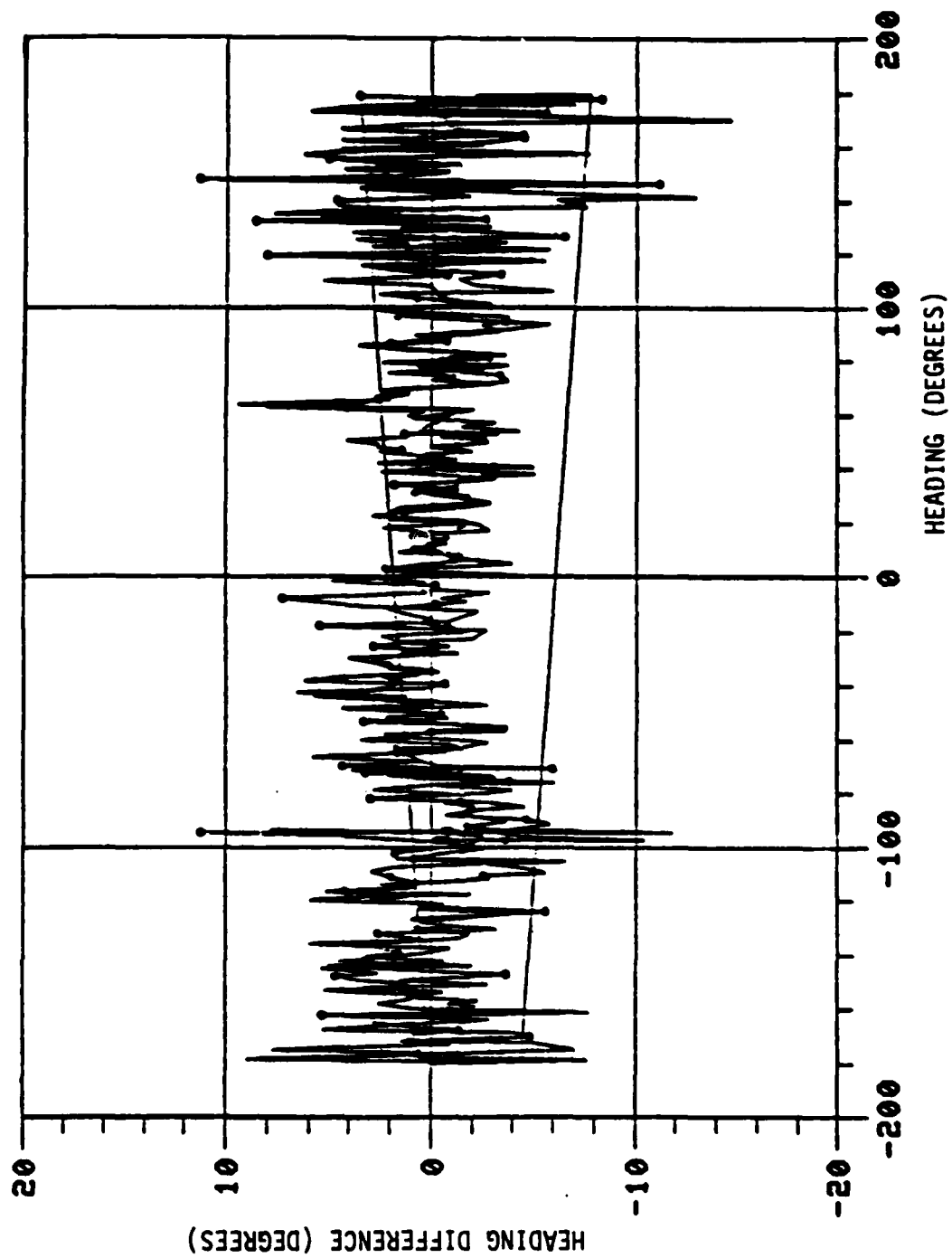


Figure 7. AFTER FULL CALIBRATION



This calibration procedure for estimating  $m_2$ ,  $m_3$  and  $m_4$  would generally be done automatically in a much more systematic (but less illustrative) way, by simply taking the first 5 terms of the Fourier series expansion of the measured function shown in figure 5.

### 3.3.0 VERTICAL POSITIONING

The vertical DR position can be defined as the barometric altitude. This is computed once every 60 seconds from a barometric pressure measurement. The pressure-height relationship in the low altitude region (0 to 11 km), can be easily derived from the standard atmosphere equations described in Reference (11) (pages 57-59) as follows:

$$P = P_0 \cdot (T/T_0)^{-g/(a \cdot R)} \quad (12)$$

$$T = T_0 + a \cdot Y \quad (13)$$

where  $P$  is the measured air pressure,  $P_0$  is the nominal sea level air pressure in the same units,  $T$  is the temperature,  $T_0$  is the defined sea level temperature of the standard atmosphere (288.16 degrees K, or 15.16 degrees C),  $a$  is the standard atmosphere temperature gradient for altitudes less than 11,000 m (about -0.0065 degrees K per metre),  $g$  is the gravitational constant (9.80665 m/s<sup>2</sup>),  $R$  is the gas constant (288 joules/(kg\*deg.K)) and  $Y$  is the vehicle height above sea level, in metres.

Substituting (13) into (12) we have:

$$P = P_0 \cdot (1 + a \cdot Y/T_0)^{-g/(a \cdot R)}$$

or

$$P = P_0 \cdot (1 + A \cdot Y)^B \quad (14)$$

where  $A$  and  $B$  are known constants with approximate values:

$$A = a/T_0 = -2.2569 \times 10^{-5} \text{ metres}^{-1}$$

$$B = -g/(a \cdot R) = 5.2386 \quad (15)$$

To obtain the barometric height  $Y$ , from the measured pressure  $P$ , equation (14) must be inverted to yield:

$$Y = \frac{e^{\left(\frac{\ln(P/P_0)}{B}\right)} - 1}{A} \quad (16)$$

The sensor chosen for the laboratory development model was a Setra Systems, Inc. High Output Pressure Transducer, model 205-2, with gage pressure range rated at 0 to 25 pounds per square inch (0 to 172 kilo-Pascals). One atmosphere is 14.7 psi (101.3 kPa), and the range of interest is roughly 11 to 16 psi (76 to 110 kPa), which corresponds to a barometric height range from about -700 metres to 2,500 metres. This barometric sensor weighs only about 100 grams and occupies only about 100 cc.

Although a pressure sensor can be expected to respond well to sudden changes in height, over longer time periods such as several hours there will be air pressure changes related to weather rather than height. (This is described in more detail in the next section). For this reason we chose to augment the barometer with a digital elevation map. The map will provide the long term (low frequency) height variations as the vehicle moves, and the baro will provide the short term (high frequency) variations. The mixing of these two height "measurements" is done in the Kalman filter, which models the errors in each system as a Markov process with the appropriate correlation time.

This digital elevation map of the Canadian arctic was created at DREO using a memory-efficient symbolic storage technique. To create this map, height above sea level was manually read directly from the 1: 1,000,000 scale topographic maps compiled in 1974 by the Surveys and Mapping Branch, Department of Energy Mines and Resources. In this way an "average" height was visually estimated for each grid square, which was one degree in longitude by one half degree in latitude. This digital map covers the region north of 60 degrees latitude and between longitudes 60 degrees west and 140 degrees west. Appendix A shows the basic map data, although it is not stored in this way. When a map height is required for a particular location (latitude, longitude) the height values, as shown on this map, are calculated for the four corners of the grid square containing this location. Two dimensional linear interpolation is then used to calculate the correct height estimate. This produces a height function that is continuous and that corresponds to the stored values on the grid corners.

This map is the only geographically limiting feature of PLANS and we hope to be able to eliminate this limitation with a global digital elevation map, or at least one covering North America and Europe.

### 3.3.1 VERTICAL ERRORS

The important vertical errors in the PLANS system are:

- v1 - inaccuracy of the pressure-height equation, due to weather
- v2 - pressure transducer error
- v3 - data communication fault
- v4 - inaccuracy of the digital elevation map

The vertical error v1 requires some explanation. The pressure-height relationship given by equation (12) describes an idealized "standard atmosphere", whereas in reality changes in weather are constantly changing the air pressure. In the Canadian Arctic, normal pressure fluctuations are (reference (12)) .1 to .2 kiloPascals over a 12 hour period, and 2.5 to 5 kPa over a half week period. This would result in a false barometric height fluctuation of 8 to 16 metres over 12 hours and 200 to 400 metres over a half week. It is possible however for extreme weather to create pressure changes of 1 kPa per hour and 10 kPa per day or, equivalently, 80 metres per hour and 800 metres per day.

The pressure transducer error v2 is claimed to be less than  $\pm .11\%FS$  (full scale), and if it is calibrated, less than  $\pm .02\%$  full scale plus  $\pm .3\%FS/deg. C$ . This amounts to an uncalibrated error of less than 15 metres in barometric height, which is very small compared with v1, so the calibration is deemed unnecessary.

V3 is meant to include any A/D conversion error, round off error, and any computational errors in evaluating equation (16).

Since the APC is presumably restricted to the earth's surface while navigating, its height above the ellipsoid is in principle a well defined function of latitude and longitude. If a sufficiently detailed elevation map could be stored in the computer's memory, then the barometer would be unnecessary and the height error v4 would not be very significant. However the map currently being used is one created at DREO with limited resources. In order for the height information to be coded and stored in an efficient manner it was necessary to quantize the heights. This vertical quantization is 50 metres for heights up to 1 km, and 100 metres for greater heights. The resulting discontinuities are removed when the map is read, by using two dimensional linear interpolation. When the map is read as a function of position the heights from the surrounding four grid squares are linearly interpolated, producing a continuous function of position. The largest error in reading this map is therefore due to the local deviation of the true height from the "area averaged" height, as visually estimated from the topographical charts. In other words, the limiting factor is the spatial resolution used to read the charts (about 60 km by 60 km) and the resolution of the charts themselves.

We estimate that our map height is accurate to approximately 30 metres plus 10% of map height (one sigma).

### 3.4.0 TRANSIT POSITIONING

Since the DR position error will generally increase without bound, an independent position fixing system is required to periodically reset the DR position. Because of its accuracy and coverage, Transit was chosen to provide these position fixes.

Transit is a satellite based navigation system, which was originally developed for the U.S. Navy Polaris submarine fleet by the Applied Physics Lab of John Hopkins University. The system has been operational since 1964, and was released for public use in 1967. Reference (14) gives a more complete description.

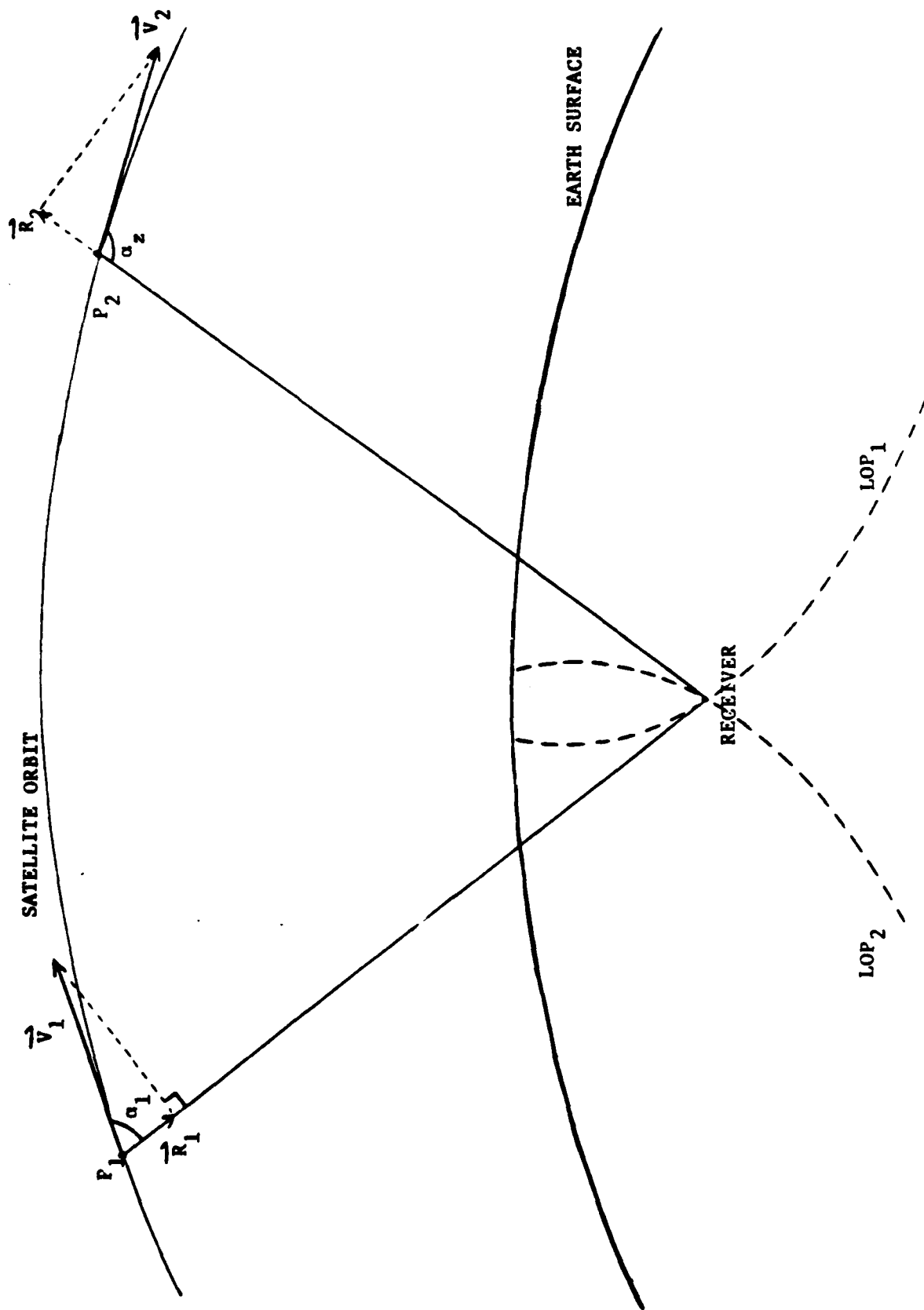
The Transit Satellite positioning system basically consists of 5 or 6 satellites in low (1,075 kilometre) circular polar orbits, with about a 107 minute period, transmitting continuously at two very stable frequencies (150 MHz and 400 MHz). An earthbound receiver can obtain a position fix whenever a satellite passes overhead, by measuring the doppler frequency shifts due to the relative motion. The transmitted signals are modulated with a data message, 6,103 bits long, at 50 bits per second. This message contains timing marks and parameters describing the satellite's orbit with enough precision to allow the receiver to accurately calculate the absolute position and velocity of the satellite. From this known satellite position and velocity profile and the doppler derived relative velocity, the receiver can calculate its own position.

The principle of operation can be explained geometrically as illustrated in Figure 8. By measuring the doppler frequency shift of the received Transit signal, the receiver can directly calculate the relative velocity of the satellite and receiver R. From the data message the receiver can calculate the satellite position P and velocity V. If the receiver is stationary then the relative velocity R is entirely due to the satellite velocity V, and satisfies the equation.

$$R = V \cos(\alpha) \quad (17)$$

where  $\alpha$  is the angle from the satellite velocity vector to the receiver. Since R and V are known, the receiver can solve equation (17) for  $\alpha$ . Therefore the receiver must be on the cone around V defined by the angle  $\alpha$ . If the receiver is known to be on the surface of the earth, then it must be on the curve defined by the intersection of the cone with the earth's surface (or a surface of known height, hence the requirement

Figure 8. TRANSIT POSITION FIX PRINCIPLE



for height input). This curve is known as a line of position (LOP). By repeating this measurement after the satellite has moved on, the receiver can obtain another LOP, and the intersection of these lines is its position. (Reference (14) gives more details).

However, to employ the position finding method described above, the receiver must either be stationary during the satellite pass, as is the case with survey instruments, or the receiver motion (velocity) relative to the earth during the pass must be known (to remove the effect of this velocity on the doppler measurement). A navigational receiver therefore must be continuously given its velocity. Any error in this velocity input will lead to an error in the position fix that the receiver produces.

Besides requiring velocity inputs, another inconvenient aspect of the Transit system is the waiting time between position fixes. This waiting time can be as short as 15 minutes or as long as 7 hours. Since the Transit satellites are in polar orbits, the mean time between fixes is shorter near the poles than at lower latitudes. Figure 9 illustrates typically how the mean time between fixes varies with latitude, from which it can be seen that in the Canadian arctic (latitude greater than 60 degrees), Transit fixes should occur on average about once every 30 to 50 minutes. This is not exact because the Transit satellite constellation geometry (orbital spacing etc.) is not kept strictly constant.

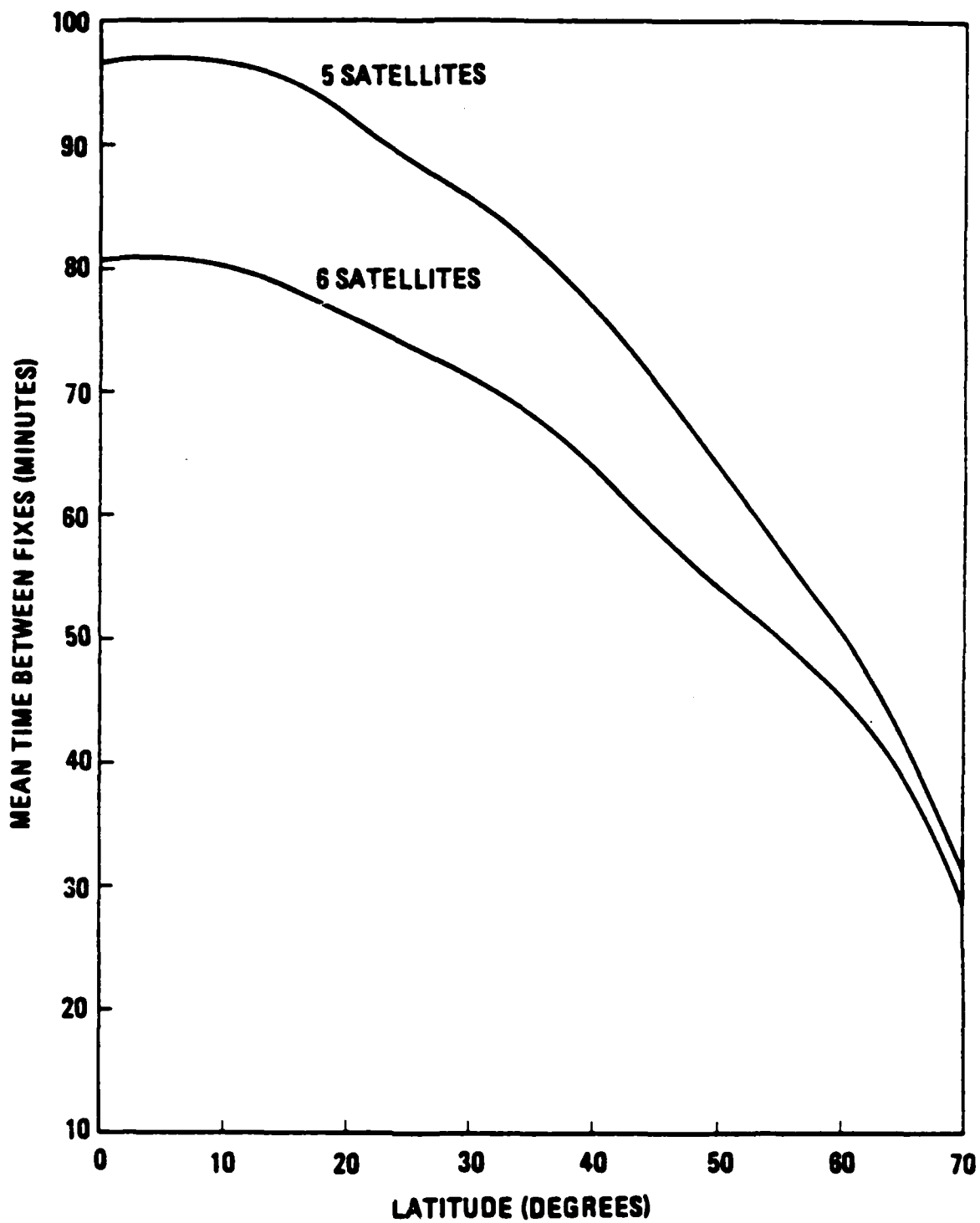
The accuracy of a Transit position fix is highly variable, depending on many factors, as is briefly explained in the following section.

#### 3.4.1 TRANSIT ERRORS

There are two basic types of Transit position errors, which can be classified as static errors and dynamic errors. The dynamic errors are caused by errors in the velocity and height information that is fed into the Transit receiver by the user, and as such can be considered to be system errors rather than just Transit errors. These dynamic errors are very important for system performance since there is no limit to their size, unless a limit can be placed on the size of the velocity and height errors. Fortunately it was possible to determine the exact relationship between velocity/height input errors and the resulting latitude/longitude output errors, the details and usefulness of which shall be described below.

The static errors are errors which will occur even if the receiver is stationary. These are fairly small but practically unavoidable, and are also described below.

Figure 9. TYPICAL MEAN TIME BETWEEN TRANSIT FIXES



#### STATIC ERRORS:

There are various sources of static errors that are not sufficiently deterministic to completely predict and compensate for:

- Ionospheric refraction
- Tropospheric refraction
- Gravitational field irregularities
- drag and radiation pressure
- clock error
- oscillator phase jitter
- ephemeris rounding error
- irregularities in the earth's motion

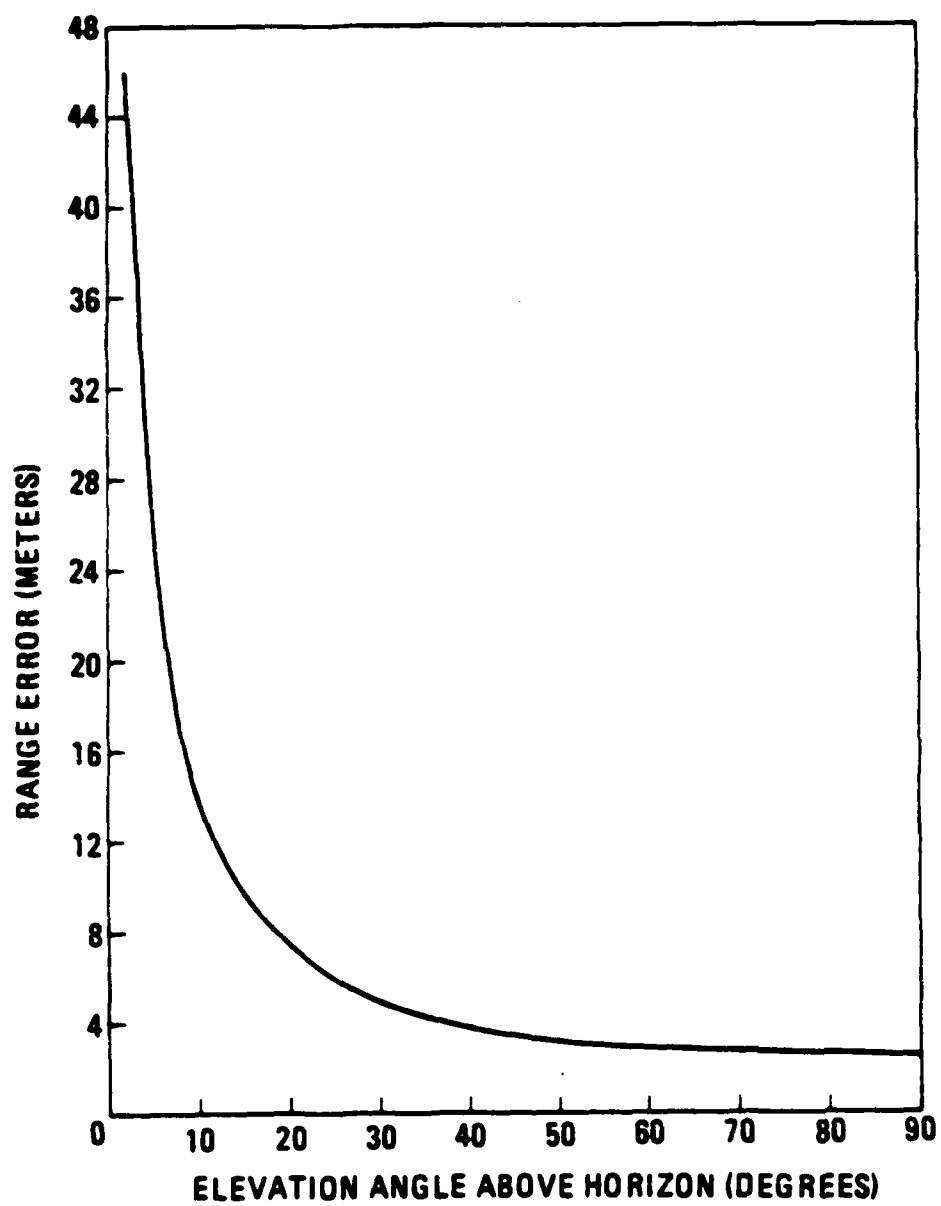
Ionospheric refraction introduces an unwanted increase in phase velocity. This results in a position error of about 90 metres in single channel receivers. Fortunately this can be largely compensated for in dual channel receivers by using the two broadcast frequencies (150 MHz and 400 MHz). Since the ionospheric wavelength stretch varies roughly quadratically with the broadcast wavelength, whereas the doppler shift is linear with frequency, these effects can be separated. The remaining refraction induced error, after compensation, is typically 1 to 5 metres.

Tropospheric refraction also introduces errors, but these are directly proportional to the frequency and thus cannot be eliminated in this way. As with many other Transit errors, the expected size of this error depends strongly on the maximum elevation angle of the satellite, (the angle from the horizon to the satellite, as seen at the receiver position) during the satellite pass. This expected tropospheric refraction error is shown in Figure 10 as a function of maximum elevation angle, where it can be seen that it is only significant (greater than 15 m) when the satellite pass has a very low maximum elevation angle of less than 10 degrees.

Further Transit position errors result from errors in the geopotential (gravity) model, and the surface force model (drag, radiation pressure) used to generate the satellite orbit. These position errors are each on the order of 10 to 30 metres.

There are other less significant but nevertheless identifiable static Transit errors, such as satellite clock error, oscillator jitter, ephemeris rounding error and unmodelled polar motion. These are all in the 1 to 5 metre range, hence not significant in our application.

Figure 10. TROPOSPHERIC REFRACTION ERROR



In summary, the total static error of the Transit position fixes will be random (uncorrelated) in direction, and its expected magnitude will depend upon the satellite elevation angle and whether the receiver is single or dual channel. Generally, the dual channel fixes will have rms position errors of about 50 metres, and single channel fixes will have errors of about 100 metres.

#### DYNAMIC ERRORS:

Reference (8) describes the exact relationship between the velocity error input and the position error output. This relationship is expressed in the form of a sensitivity matrix H, where:

$$\begin{pmatrix} \text{north position error} \\ \text{east position error} \end{pmatrix} = \begin{pmatrix} h_{11} & h_{12} \\ h_{21} & h_{22} \end{pmatrix} * \begin{pmatrix} \text{north velocity error} \\ \text{east velocity error} \end{pmatrix} \quad (18)$$

As is shown in reference (8), the components of this sensitivity matrix H are complicated functions of the satellite maximum elevation angle, the satellite direction of travel (north to south or vice versa), the receiver latitude, and whether the satellite subpoint is east or west of the receiver at maximum elevation. These are not easily expressed in closed form, but an algorithm to evaluate them has been implemented in the PLANS processor. Figure 11 illustrates the magnitudes of the north and east components of the position error (DN, DE), induced by a 1 metre per second velocity error in the north direction. These position errors are shown as functions of satellite elevation angle, for a particular receiver latitude and satellite direction of travel. Figure 12 shows the position error components due to an east velocity error.

The important fact to be drawn from equation (18) is that it is deterministic and linear in the velocity error. Therefore if there is more uncertainty in the velocity than in the position, equation (18) can be inverted to solve for the velocity error. The Kalman filter effectively does this automatically in PLANS, thereby limiting the velocity uncertainty which otherwise would be unlimited because of the heading error in directional gyro mode, especially near the magnetic pole.

An error in the height supplied to the receiver also produces a Transit position error that can be defined as a function of the same parameters used in the H matrix above. This is also derived in reference (8), but it can be more easily expressed in closed form: The north and east position error dN and dE (true position - Transit position), due to a height error dH (true height - height estimate), can be expressed as

FIGURE 11. TRANSIT POSITION ERROR DUE TO NORTH INPUT VELOCITY ERROR.

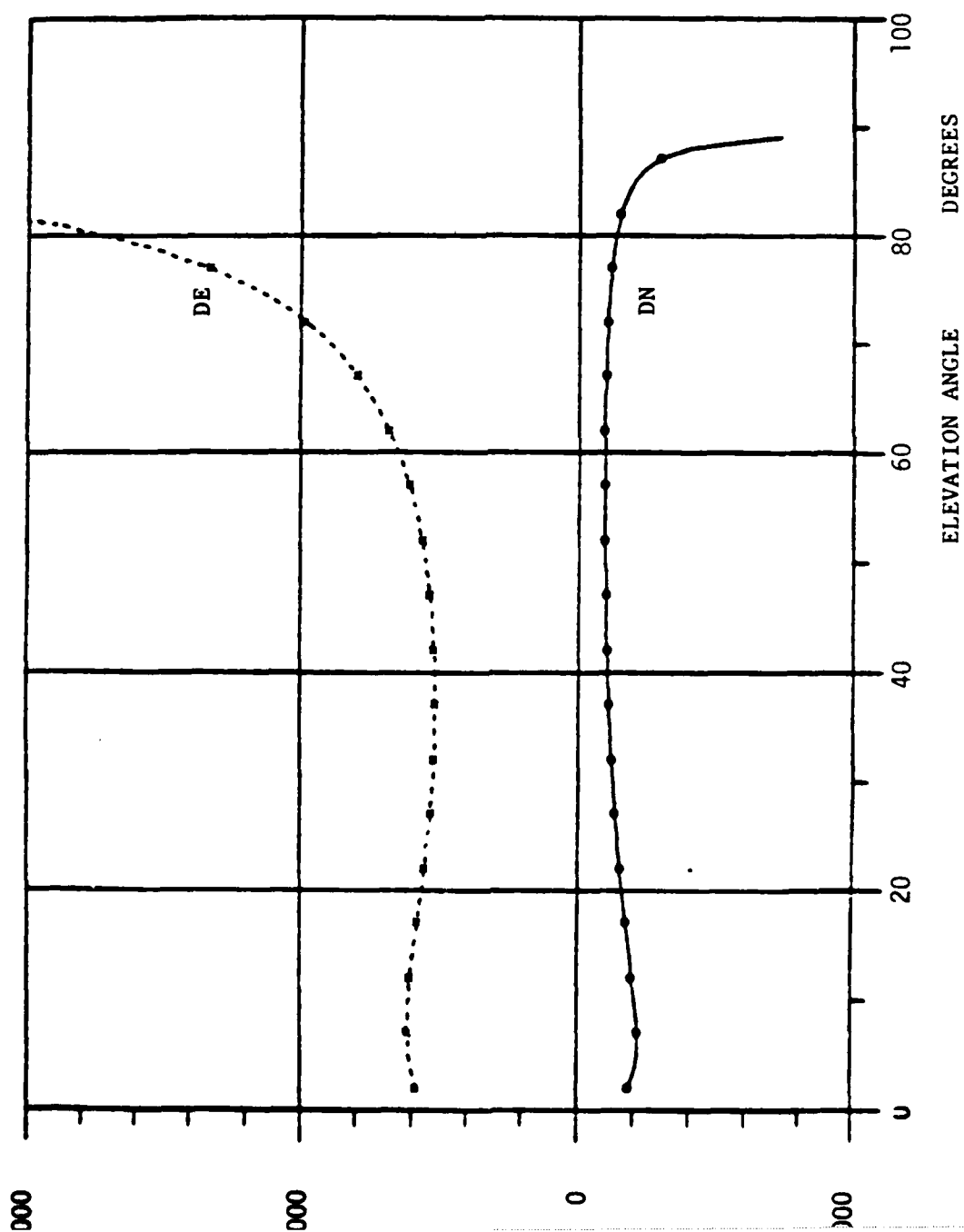
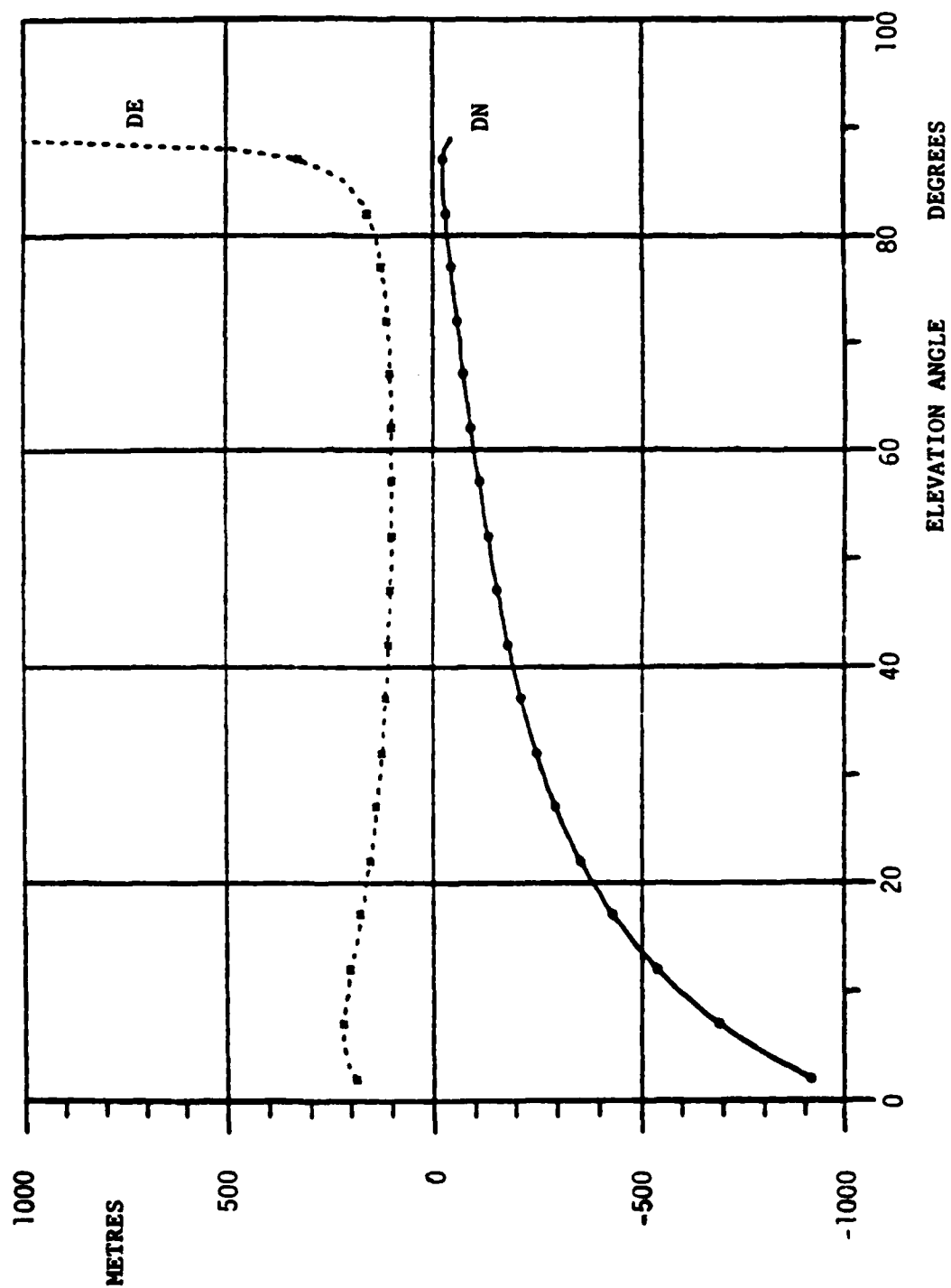


FIGURE 12. TRANSIT POSITION ERROR DUE TO EAST INPUT VELOCITY ERROR.



$$\begin{pmatrix} dN \\ dE \end{pmatrix} = \begin{pmatrix} \cos(\Psi) \tan(\sigma) \\ \sin(\Psi) \tan(\sigma) \end{pmatrix} dH \quad (19)$$

where  $\sigma$  is the satellite maximum elevation angle, which the receiver supplies, and  $\Psi$  is the bearing from the receiver to the satellite subpoint (at closest approach) which can be computed from  $\sigma$ , the direction of travel, and the receiver position. Equation (19) is derived in reference (8). The magnitude of this error is illustrated in Figure 13, which shows the position error induced by a 100 metre height error, for a particular receiver latitude and satellite direction of travel.

It is important to notice that, like equation (18), equation (19) is also deterministic and is linear in the height error. The errors described by equations (18) and (19) are in fact independent of each other and of the static errors. These errors are all additive, so that the total Transit position fix error can be expressed as:

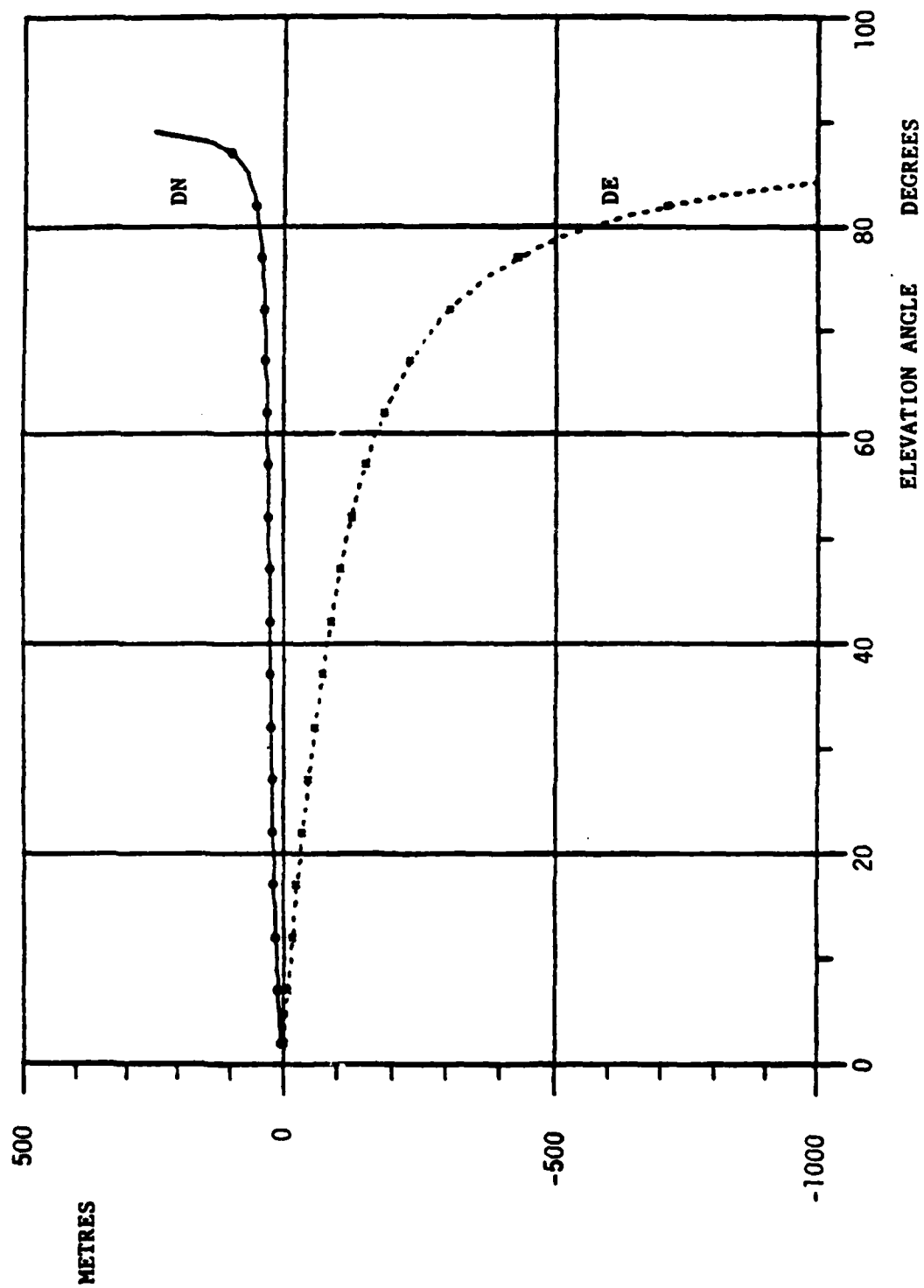
$$\begin{pmatrix} dN \\ dE \end{pmatrix} = \begin{pmatrix} \cos(\Psi) \tan(\sigma) & h11 & h12 \\ \sin(\Psi) \tan(\sigma) & h21 & h22 \end{pmatrix} \begin{pmatrix} dH \\ dVn \\ dVe \end{pmatrix} + \begin{pmatrix} s1 \\ s2 \end{pmatrix} \quad (20)$$

where  $dVn$  and  $dVe$  are the velocity error components and  $s1$  and  $s2$  are the static position error components.

### 3.5.0 GPS POSITIONING

The Global Positioning System (GPS) is a satellite based navigation system that has not yet (as of 1985) been fully implemented. It should be fully operational by about 1989. It will consist of 18 satellites in 6 orbits at a height of 20,200 Km., with orbital inclination of 55 degrees and period of 12 hours. There will also be a ground control segment and two basic types of receiver equipment, precise or "p-code" receivers for military use, and course acquisition or "C/A-code" receivers for civilian or low cost applications. Each satellite will continually broadcast coded messages at two frequencies (1,227.6 MHz and 1,575.4 MHz). The P-code receivers will be able to decode both messages, whereas the C/A-code receivers will only be able to decode one. This system is designed to provide highly accurate 3 dimensional position, 3 dimensional velocity, and time measurements, continuously, on a worldwide basis, with high dynamic capability.

FIGURE 13: TRANSIT POSITION ERROR DUE TO INPUT HEIGHT ERROR



The Magnovox Transit receiver that we have chosen for PLANS, the MX1107, has the ability to be easily upgraded to include a C/A-code GPS receiver. The existing satellite constellation provides about 5 to 6 hours of coverage per day, in two segments 12 hours apart. This varies with receiver location, and will be expanding as more satellites are launched. Even these two short periods will provide the PLANS system with a significant improvement by bounding the accumulated position and velocity error and by calibrating the drift rates.

### 3.5.1 GPS ERRORS

At present the GPS errors are quite small compared to the other system errors, and are largely uncorrelated. Therefore it is not necessary to provide a detailed stochastic model for these errors. They can be simply treated as additive white noise in the Kalman filter measurement process. The p-code accuracy will be about 15 metres in position (SEP), .1 metre/second in velocity and .1 microsecond in time. Reference(15) describes the GPS system in more detail.

The MX1107 has a C/A-code GPS receiver which claims to have a horizontal accuracy of 50 metres or better, at a 90% probability level, at an HDOP (horizontal dilution of precision) of 3.0. Since the receiver provides the numerical values of this geometric dilution of precision in each direction, these numbers shall be used as scale factors in the Kalman filters error model.

#### 4.0 COMPUTER

Central to the PLANS navigation system is a digital computer on which to implement the large amount of necessary software. For the PLANS computer a Motorola 68000 microprocessor was selected. This is a second generation 16-bit microprocessor, which comes on a 64 pin chip. This processor has 61 basic instructions, 14 addressing modes, 16 general purpose registers (32 bits each) and can directly address 16 megabytes. In practice this resembles a classical minicomputer. It is presently mounted on a printed circuit board of standard Eurocard format (160 mm by 234mm) along with 32K bytes of RAM (random access memory), 128 k bytes of EPROM (erasable programmable read only memory) and an RS232C serial port. The PLANS computer consists of this card along with three other full-sized cards and five half-sized cards, mounted in a box as shown in Figure 14. These other cards contain the necessary memory, floating point hardware and interfaces for communication with the keyboard, displays and sensors. Two of these cards (6 and 7) are described in more detail in references (17) and (18).

Full boards: 1/ MC68000 + (32K RAM and 128K EPROM) + RS232 serial port (VME BUS)

2/ 256K bytes dynamic RAM

3/ up to 512 K bytes EPROM

4/ floating point processor

Half boards: 5/ analog to digital converters (8 differential channels) (I/O channel)

6/ serial ports (four RS232C or RS422A ports)

7/ digital ports (various)

8/ analog circuits (signal conditioning)

9/ synchro to digital converter

In production of course it will be possible to greatly reduce the number of boards required for the processor, memory and interfaces. By using higher density memory and so on, it should be possible to combine all of these boards into one.

Of course a keypad and display are also required for operator interaction. For the initial testing a standard video terminal with a full keyboard has been used (a CIT 101). This will be replaced by a small keypad (4 by 5 keys) and a custom made LCD display, which has been developed to DREO specifications by Data Images Inc. of Ottawa. There will also be two small remote LCD displays for the driver and the commander.

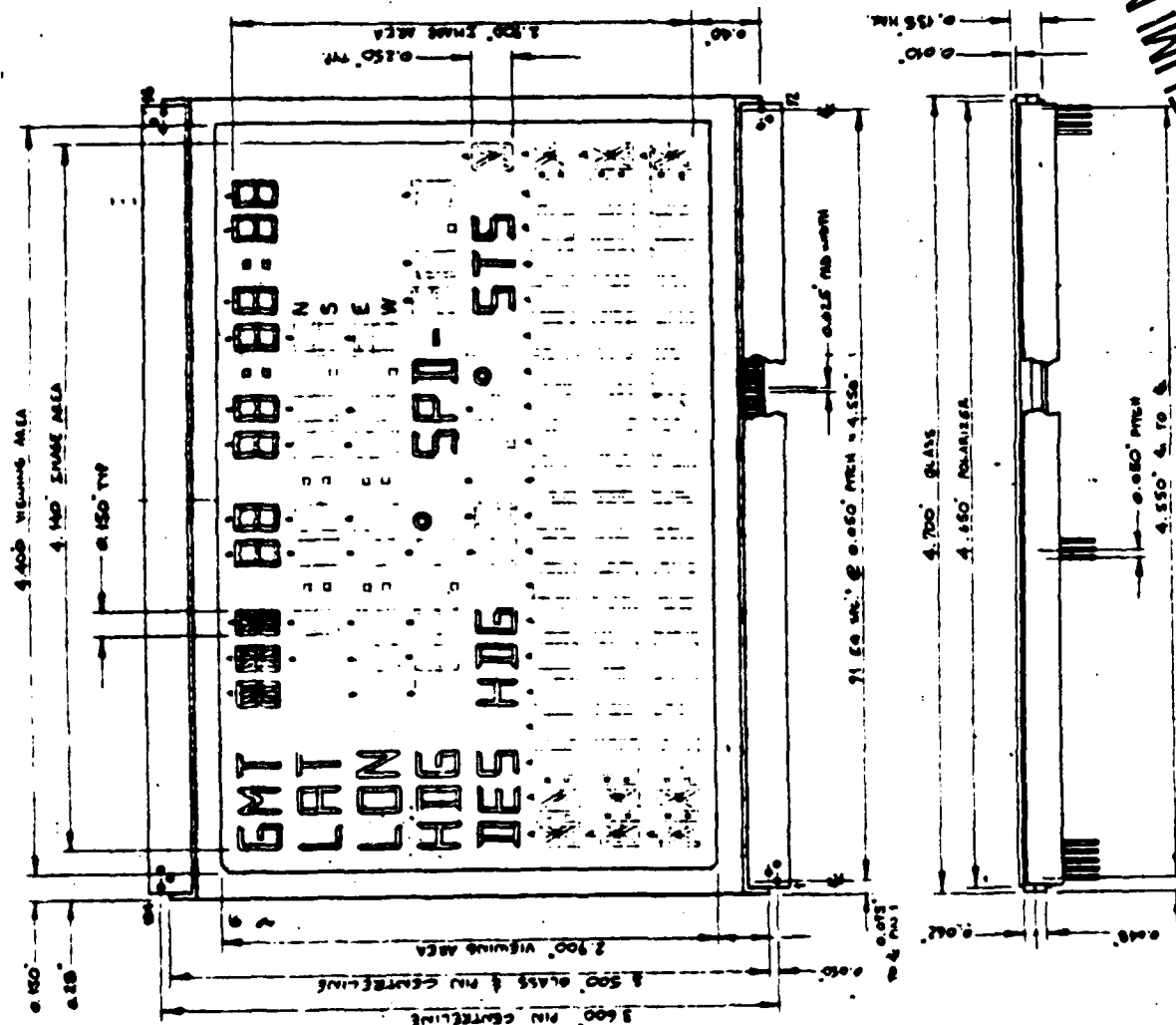
Figure 14. PLANS PROCESSOR CONFIGURATION

GENERAL INTERFACE	SYNCHRO to DIGITAL
4 SERIAL PORTS	
ANALOG BOARD	ANALOG to DIGITAL
SPARE	SPARE
MOTOROLA 68000 MICROPROCESSOR	
RAM	
EPROM	
FLOATING POINT PROCESSOR	
EPROM	
MAGNAVOX MX1107R  TWO CHANNEL TRANSIT  PLUS C/A CODE GPS	
POWER SUPPLIES	

## 5.0 DISPLAYS

The main display, sketched in Figure 15, is a transflective (backlit and reflective) custom made LCD display, about 3" by 4.5" in size, to be used in conjunction with a 4 by 5 keypad to control the system. It will constantly show the time (Greenwich Mean Time), best estimates of latitude and longitude (in WGS-72 coordinates), heading in degrees clockwise from north, and speed in kilometers per hour. This main display also shows a desired heading and a status character, and has three 20 character lines for general use, such as to echo keypad inputs, show helpful messages, display waypoint information, UTM coordinates, etc.

The remote display, sketched in Figure 16, also shows the latitude, longitude and heading estimates. In addition it has a large "bow-tie" heading-to-steer indicator to assist in track-keeping or waypoint following. If the vehicle is off course, the appropriate segments will light up to create an arrow pointing in the direction to steer, of a size proportional to the size of the course deviation (the difference between the actual and desired heading). A further numeric field is switch selectable to show either the desired heading or the course deviation.



**1.400. VERNUM A&A**

4. 140' INLAND AREA

— aiso'rw

GMT 167  
LAT 167  
LON 50H  
HQS 50H  
DES 50H  
515  
SPD-045  
W  
S  
N

500 CLASS & IN CENTERLINE  
500 IN CENTERLINE

2.00 VISUAL AREA

7200 10000 0000  
100 0000 0000

1.000 CLASS

**000000**

5 NW 009

104 000

425. Old South

11 20 W. @ 0.050' AREA = 4.550"

0.075

1. 700' 92.135

1:550' POLARIS 2.6A

— 0.050" PWT

**4.550' 6 to 8**

**4.550' 6 to 8**

**DRAWING PRELIMINARY**

**Notes:**

A - DOWTES 10 SEC. SUPRA-SONIC CHAS.  
B - DOWTES 7 SEC. MONTAG CHAS.  
-- SEE DOW. C-192 ABOUT 2 FOR HYDRAUL.  
ELECTRICAL CONNECTIONS.

**DO NOT SCALE DRAWINGS**

CUSTOM - L.C.D. (CHECK DISTAL)

100

11-17-68

10

Figure 16. REMOTE DISPLAY

**# DO NOT SCALE DRAWING**

**DESCRIPTION:**  
**CUSTOM - LCD.**

DATE	11 MAR 81	FILE	2-1
BY	DR	SCALE	2-1
REVISION	1	DATE	11 MAR 81
REVISION	2	DATE	11 MAR 81
REVISION	3	DATE	11 MAR 81
REVISION	4	DATE	11 MAR 81
REVISION	5	DATE	11 MAR 81
REVISION	6	DATE	11 MAR 81
REVISION	7	DATE	11 MAR 81
REVISION	8	DATE	11 MAR 81
REVISION	9	DATE	11 MAR 81
REVISION	10	DATE	11 MAR 81
REVISION	11	DATE	11 MAR 81
REVISION	12	DATE	11 MAR 81
REVISION	13	DATE	11 MAR 81
REVISION	14	DATE	11 MAR 81
REVISION	15	DATE	11 MAR 81
REVISION	16	DATE	11 MAR 81
REVISION	17	DATE	11 MAR 81
REVISION	18	DATE	11 MAR 81
REVISION	19	DATE	11 MAR 81
REVISION	20	DATE	11 MAR 81
REVISION	21	DATE	11 MAR 81
REVISION	22	DATE	11 MAR 81
REVISION	23	DATE	11 MAR 81
REVISION	24	DATE	11 MAR 81
REVISION	25	DATE	11 MAR 81
REVISION	26	DATE	11 MAR 81
REVISION	27	DATE	11 MAR 81
REVISION	28	DATE	11 MAR 81
REVISION	29	DATE	11 MAR 81
REVISION	30	DATE	11 MAR 81
REVISION	31	DATE	11 MAR 81
REVISION	32	DATE	11 MAR 81
REVISION	33	DATE	11 MAR 81
REVISION	34	DATE	11 MAR 81
REVISION	35	DATE	11 MAR 81
REVISION	36	DATE	11 MAR 81
REVISION	37	DATE	11 MAR 81
REVISION	38	DATE	11 MAR 81
REVISION	39	DATE	11 MAR 81
REVISION	40	DATE	11 MAR 81
REVISION	41	DATE	11 MAR 81
REVISION	42	DATE	11 MAR 81
REVISION	43	DATE	11 MAR 81
REVISION	44	DATE	11 MAR 81
REVISION	45	DATE	11 MAR 81
REVISION	46	DATE	11 MAR 81
REVISION	47	DATE	11 MAR 81
REVISION	48	DATE	11 MAR 81
REVISION	49	DATE	11 MAR 81
REVISION	50	DATE	11 MAR 81
REVISION	51	DATE	11 MAR 81
REVISION	52	DATE	11 MAR 81
REVISION	53	DATE	11 MAR 81
REVISION	54	DATE	11 MAR 81
REVISION	55	DATE	11 MAR 81
REVISION	56	DATE	11 MAR 81
REVISION	57	DATE	11 MAR 81
REVISION	58	DATE	11 MAR 81
REVISION	59	DATE	11 MAR 81
REVISION	60	DATE	11 MAR 81
REVISION	61	DATE	11 MAR 81
REVISION	62	DATE	11 MAR 81
REVISION	63	DATE	11 MAR 81
REVISION	64	DATE	11 MAR 81
REVISION	65	DATE	11 MAR 81
REVISION	66	DATE	11 MAR 81
REVISION	67	DATE	11 MAR 81
REVISION	68	DATE	11 MAR 81
REVISION	69	DATE	11 MAR 81
REVISION	70	DATE	11 MAR 81
REVISION	71	DATE	11 MAR 81
REVISION	72	DATE	11 MAR 81
REVISION	73	DATE	11 MAR 81
REVISION	74	DATE	11 MAR 81
REVISION	75	DATE	11 MAR 81
REVISION	76	DATE	11 MAR 81
REVISION	77	DATE	11 MAR 81
REVISION	78	DATE	11 MAR 81
REVISION	79	DATE	11 MAR 81
REVISION	80	DATE	11 MAR 81
REVISION	81	DATE	11 MAR 81
REVISION	82	DATE	11 MAR 81
REVISION	83	DATE	11 MAR 81
REVISION	84	DATE	11 MAR 81
REVISION	85	DATE	11 MAR 81
REVISION	86	DATE	11 MAR 81
REVISION	87	DATE	11 MAR 81
REVISION	88	DATE	11 MAR 81
REVISION	89	DATE	11 MAR 81
REVISION	90	DATE	11 MAR 81
REVISION	91	DATE	11 MAR 81
REVISION	92	DATE	11 MAR 81
REVISION	93	DATE	11 MAR 81
REVISION	94	DATE	11 MAR 81
REVISION	95	DATE	11 MAR 81
REVISION	96	DATE	11

TRUTH TABLE - LOWER ROW CHARACTERS & INDICATOR

TR:5TH TABLE - UPPER, ROW CHARACTERS

	1	2	3	4	5	6	7	8	9	10	11	12	13	14	15	16	17	18	19	20	21	22	23	24	25	26	27	28	29	30
Ph2																														
Ph3																														
Ph4																														
Ph5																														
Ph6																														
Ph7																														
Ph8																														
Ph9																														
Ph10																														
Ph11																														
Ph12																														
Ph13																														
Ph14																														
Ph15																														
Ph16																														
Ph17																														
Ph18																														
Ph19																														
Ph20																														
Ph21																														
Ph22																														
Ph23																														
Ph24																														
Ph25																														
Ph26																														
Ph27																														
Ph28																														
Ph29																														
Ph30																														
Ph31																														
Ph32																														
Ph33																														
Ph34																														
Ph35																														
Ph36																														
Ph37																														
Ph38																														
Ph39																														
Ph40																														
Ph41																														
Ph42																														
Ph43																														
Ph44																														
Ph45																														
Ph46																														
Ph47																														
Ph48																														
Ph49																														
Ph50																														
Ph51																														
Ph52																														
Ph53																														
Ph54																														
Ph55																														
Ph56																														
Ph57																														
Ph58																														
Ph59																														
Ph60																														
Ph61																														
Ph62																														
Ph63																														
Ph64																														
Ph65																														
Ph66																														
Ph67																														
Ph68																														
Ph69																														
Ph70																														
Ph71																														
Ph72																														
Ph73																														
Ph74																														
Ph75																														
Ph76																														
Ph77																														
Ph78																														
Ph79																														
Ph80																														
Ph81																														
Ph82																														
Ph83																														
Ph84																														
Ph85																														
Ph86																														
Ph87																														
Ph88																														
Ph89																														
Ph90																														
Ph91																														
Ph92																														
Ph93																														
Ph94																														

PRO- CESS	50	40	30	20	10	0	42	41	40	39	38	37	36	35	34	33	32	31	30	29	28	27	26	25	24	23	22	21	20	19	18	17	16	15	14	13	12	11	10	9	8	7	6	5	4	3	2	1	0		
1	100	90	80	70	60	50	40	30	20	10	0	10	20	30	40	50	60	70	80	90	100	90	80	70	60	50	40	30	20	10	0	10	20	30	40	50	60	70	80	90	100	90	80	70	60	50	40	30	20	10	0
2	100	90	80	70	60	50	40	30	20	10	0	10	20	30	40	50	60	70	80	90	100	90	80	70	60	50	40	30	20	10	0	10	20	30	40	50	60	70	80	90	100	90	80	70	60	50	40	30	20	10	0
3	100	90	80	70	60	50	40	30	20	10	0	10	20	30	40	50	60	70	80	90	100	90	80	70	60	50	40	30	20	10	0	10	20	30	40	50	60	70	80	90	100	90	80	70	60	50	40	30	20	10	0
4	100	90	80	70	60	50	40	30	20	10	0	10	20	30	40	50	60	70	80	90	100	90	80	70	60	50	40	30	20	10	0	10	20	30	40	50	60	70	80	90	100	90	80	70	60	50	40	30	20	10	0
5	100	90	80	70	60	50	40	30	20	10	0	10	20	30	40	50	60	70	80	90	100	90	80	70	60	50	40	30	20	10	0	10	20	30	40	50	60	70	80	90	100	90	80	70	60	50	40	30	20	10	0
6	100	90	80	70	60	50	40	30	20	10	0	10	20	30	40	50	60	70	80	90	100	90	80	70	60	50	40	30	20	10	0	10	20	30	40	50	60	70	80	90	100	90	80	70	60	50	40	30	20	10	0
7	100	90	80	70	60	50	40	30	20	10	0	10	20	30	40	50	60	70	80	90	100	90	80	70	60	50	40	30	20	10	0	10	20	30	40	50	60	70	80	90	100	90	80	70	60	50	40	30	20	10	0
8	100	90	80	70	60	50	40	30	20	10	0	10	20	30	40	50	60	70	80	90	100	90	80	70	60	50	40	30	20	10	0	10	20	30	40	50	60	70	80	90	100	90	80	70	60	50	40	30	20	10	0
9	100	90	80	70	60	50	40	30	20	10	0	10	20	30	40	50	60	70	80	90	100	90	80	70	60	50	40	30	20	10	0	10	20	30	40	50	60	70	80	90	100	90	80	70	60	50	40	30	20	10	0

## 6.0 KALMAN FILTER DESIGN

It is primarily the errors of the dead reckoning system that the Kalman filter estimates. That is, the north and east position error (in metres), the gyrocompass heading error (in radians), the vehicle odometer scale factor error (dimensionless) and the baroaltimeter height error (metres). In directional gyro mode, the gyro drift rate is also modelled. The Kalman filter also estimates the correlated errors of the aiding sensors, such as the magnetic flux valve heading error (radians) and the error of the digital map height (metres).

The filter estimates these errors by processing all of the available measurements using suitable stochastic and deterministic error models. Reference (16) describes the standard stochastic model types and provides an elementary introduction to Kalman filtering techniques.

### 6.1 STATE VECTOR

The PLANS filter employs an eight dimensional state space. The eight states have been defined as follows:

$$\begin{matrix} x1 \\ x2 \\ x3 \\ x4 \\ x5 \\ x6 \\ x7 \\ x8 \end{matrix} = \begin{matrix} \text{true height above geoid} & - & \text{map height} \\ \text{true height above geoid} & - & \text{baroaltimeter height} \\ \text{true heading} & - & \text{magnetic heading} \\ \text{gyro drift rate when in directional gyro mode} & & \\ \text{true heading} & - & \text{gyro heading} \\ (\text{true speed} & - & \text{odometer speed})/\text{odometer speed} \\ (\text{true latitude} & - & \text{DR latitude}) \text{ (in metres)} \\ (\text{true longitude} & - & \text{DR longitude}) \text{ (in metres)} \end{matrix} \quad (21)$$

It should be clarified that these states represent the markov, or time correlated portions of the errors. The uncorrelated component of the sensor errors are treated as measurement noise. The units and sign conventions are as follows:

$$\begin{matrix} \text{metres} \\ \text{metres} \\ \text{radians} \\ \text{radians/second} \\ \text{radians} \\ \text{dimensionless} \\ \text{metres} \\ \text{metres} \end{matrix} \quad \begin{matrix} +\text{ve up} \\ +\text{ve up} \\ +\text{ve clockwise from true north} \\ +\text{ve clockwise from true north} \\ +\text{ve clockwise from true north} \\ +\text{ve to vehicle front} \\ +\text{ve north} \\ +\text{ve east} \end{matrix} \quad (22)$$

There are actually two state vectors involved, because state  $x4$  is deleted when in gyrocompass mode.

## 6.2 TRANSITION MATRIX

The DR position error is simply the integral of the DR velocity error. This fact, together with the assumed stochastic error models for the DR velocity errors and the remaining state vector components, is used to propagate the state vector in time, according to the vector differential equation:

$$\dot{X}(t) = F(t)*X(t) + W(t) \quad (23)$$

This is used to propagate  $X$  between measurements. To implement this on a digital computer, equation (23) was converted to a discrete difference equation and linearized, to obtain the STATE TRANSITION matrix  $\Phi$ , where:

$$X(t+dt) = \Phi X(t) + W(dt) \quad (24)$$

The result is

$$\begin{pmatrix} X1 \\ X2 \\ X3 \\ X4 \\ X5 \\ X6 \\ X7 \\ X8 \end{pmatrix} = \begin{pmatrix} e^{-dt/T1} & & & & & & & \\ & e^{-dt/T2} & & & & & & \\ & & e^{-dt/T3} & & & & & \\ & & & \boxed{\phantom{000000}} & & & & \\ & & & & & & & \\ & & & & & e^{-dt/T6} & & \\ & & & & & & \Phi(7,5) & \Phi(7,6) & 1 & 0 \\ & & & & & & \Phi(8,5) & \Phi(8,6) & 0 & 1 \end{pmatrix} \begin{pmatrix} X1 \\ X2 \\ X3 \\ X4 \\ X5 \\ X6 \\ X7 \\ X8 \end{pmatrix} + \begin{pmatrix} W1 \\ W2 \\ W3 \\ W4 \\ W5 \\ W6 \\ 0 \\ 0 \end{pmatrix} \quad (25)$$

where:

$$\begin{aligned} \Phi(7,5) &= -dt*S*\sin(\theta + x5/2) \\ \Phi(7,6) &= dt*S*\cos(\theta + x5) \\ \Phi(8,5) &= dt*S*\cos(\theta + x5/2) \\ \Phi(8,6) &= dt*S*\sin(\theta + x5) \end{aligned} \quad (26)$$

where  $dt$  is the propagation time interval,  $S$  is the deadreckoning speed,  $\theta$  is the deadreckoning heading, and the submatrix:

$$\begin{aligned}
 & \begin{bmatrix} & & & & & \\ & & & & & \\ & & & & & \\ & & & & & \\ & & & & & \\ & & & & & \end{bmatrix} = \begin{bmatrix} -dt/T4 & & & & & \\ e & & & & 0 & \\ & -dt/T4 & & & & \\ T4(1-e & & & & & \\ & & & & & \\ & & & & & 1 \end{bmatrix} \quad \text{in directional gyro mode} \\
 & \begin{bmatrix} & & & & & \\ & & & & & \\ & & & & & \\ & & & & & \\ & & & & & \\ & & & & & \end{bmatrix} = \begin{bmatrix} 0 & & 0 & & & \\ & & & & & \\ & & & -dt/T5 & & \\ 0 & & e & & & \end{bmatrix} \quad \text{in gyrocompass mode}
 \end{aligned} \tag{27}$$

where:

- T1 = map height error correlation time
- T2 = baroaltimeter height error correlation time
- T3 = magnetic declination error correlation time
- T4 = gyro drift rate correlation time
- T5 = gyro markov error correlation time
- T6 = odometer speed factor error correlation time

(28)

and

Wi = driving white noise with covariance Qi

where (see page 82 reference (16)):

$$Q_i = M_i * (1 - e^{-2*dt/T_i}) \tag{29}$$

where the Mi are the markov process steady state root mean squared values:

- M1 = map height error covariance
- M2 = baroaltimeter height error covariance
- M3 = magnetic declination error covariance
- M4 = gyro drift rate covariance
- M5 = gyro heading error covariance
- M6 = speed factor error covariance.

(30)

Numerical values for Ti and Mi (i=1 to 6) are given in Appendix C.

Notice from equations (25) and (26) that the state transition equation has not been completely linearized in  $X$ , and consequently the transition matrix  $\Phi$  still exhibits a weak dependence on the state vector  $X$ . Therefore this PLANS design uses an extended Kalman filter rather than a simple linear one. This is necessary because of the potentially large deadreckoning heading error,  $X_5$ , that could occur in directional gyro mode, and the fact that the DR position error,  $(X_7, X_8)$ , varies nonlinearly with this heading error.

This nonlinearity in heading and potentially large heading error also forced us to adopt a closed loop filter design whereby we fed the filtered estimate of velocity and height into the Transit receiver.

### 6.3 MEASUREMENT VECTOR

The odometer "speed" and gyro heading are measured at a 1 Hz rate for dead reckoning, and the digital map is read once a minute to obtain the height. The filter measures the baroaltimeter and the magnetic flux valve once a minute to update its estimate of the state vector  $X$  (especially  $X_1$ ,  $X_2$  and  $X_3$ ). Transit position fixes are processed whenever they occur to update the filter estimate of  $X$  (especially  $X_7$  and  $X_8$  but also  $X_5$  and  $X_6$ ). Whenever the vehicle is in directional gyro mode and is not moving, the gyro drift rate is measured from successive heading measurements, to allow the filter to update the estimate of  $X_4$ . When GPS coverage allows, three dimensional position, horizontal velocity and time measurements will be made at a rate of at least once per minute. This time measurement is independent of the chosen state vector, but the position and velocity measurements will strongly affect the state vector.

The Kalman filter's measurement vector is therefore defined as:

$$\begin{array}{lcl} \begin{array}{l} z_1 \\ z_2 \\ z_3 \\ z_4 \\ z_5 \\ z_6 \\ z_7 \\ z_8 \\ z_9 \\ z_{10} \end{array} & = & \begin{array}{l} \begin{array}{l} \text{map height} \\ \text{map height} \\ \text{magnetic heading} \\ (\text{gyro heading}(t+dt) \\ \text{Transit latitude} \\ \text{Transit longitude} \\ \text{GPS latitude} \\ \text{GPS longitude} \\ \text{GPS north velocity} \\ \text{GPS east velocity} \end{array} \\ \begin{array}{l} - \\ - \\ - \\ - \\ - \\ - \\ - \\ - \\ - \\ - \end{array} \\ \begin{array}{l} \text{barometric height} \\ \text{GPS height} \\ \text{gyro heading} \\ \text{gyro heading}(t) / dt \\ \text{DR latitude (in metres)} \\ \text{DR longitude (in metres)} \\ \text{DR latitude (in metres)} \\ \text{DR longitude (in metres)} \\ \text{DR north velocity} \\ \text{DR east velocity} \end{array} \end{array} \quad (31)$$

The units and collection rates are:

$$\begin{array}{lcl} \begin{array}{l} \text{metres} \\ \text{metres} \\ \text{radians} \\ \text{radians/second} \\ \text{metres} \\ \text{metres} \\ \text{metres} \\ \text{metres} \\ \text{metres/second} \\ \text{metres/second} \end{array} & & \begin{array}{l} 1 \text{ minute} \\ 30 \text{ sec.} \\ 1 \text{ minute} \\ 1 \text{ minute (while stationary \& in DG mode)} \\ \sim 50 \text{ minutes (at 60 degrees latitude)} \\ \sim 50 \text{ minutes (at 60 degrees latitude)} \\ 30. \text{ sec.} \\ 30. \text{ sec.} \\ 30. \text{ sec.} \\ 30. \text{ sec.} \end{array} \quad (32)$$

The Transit position fixes occur at irregular intervals, averaging about once every 90 minutes at low latitudes and more frequently at higher latitudes, as shown in Figure 6. A Transit height measurement may also be available under special conditions.

It should be mentioned that, in order to be at all useful at high latitudes, the raw magnetic flux valve measurement must first be adjusted using a magnetic declination value. The PLANS software generates this magnetic declination using the IGRF80A geomagnetic field model, described in reference (5). This field model predicts all three components of the earth's magnetic field, which allows not only the magnetic declination to be calculated, but also the horizontal field strength and the dip angle, which can be used to give a reasonable indication of the accuracy that can be expected from the flux valve. The magnetic heading measurements are also adjusted using the calibration function described in section 3.2.2, which corrects for the permanent and induced fields of the vehicle.

When GPS has been incorporated the measurement vector will be expanded to include the two position error measurements (GPS - DR) shown, as well as perhaps two velocity error measurements, a height error measurement and a time measurement whenever a sufficient number of GPS satellites are "visible".

#### 6.4 MEASUREMENT MATRIX

The relationship between the state vector  $X$  and the measurement vector  $z$  must be described in detail for the Kalman filter to properly process the measurements. This description is expressed as a measurement equation:

$$Z = H * X + V \quad (33)$$

where  $H$  is the "measurement matrix" and  $V$  is the measurement noise vector. For PLANS the measurement equation is:

$$Z = \begin{pmatrix} -1 & 1 & & & & & & & & \\ -1 & 0 & & & & & & & & \\ & & -1 & 0 & 1 & & & & & \\ & & 0 & -1 & 0 & & & & & \\ H51 & 0 & 0 & 0 & H55 & H56 & 1 & 0 & & \\ H61 & 0 & 0 & 0 & H65 & H66 & 0 & 1 & & \\ & & & & & & 1 & 0 & & \\ & & & & & & 0 & 1 & & \\ & & & & -S \sin \theta & S \cos \theta & & & & \\ & & & & S \cos \theta & S \sin \theta & & & & \end{pmatrix} \begin{pmatrix} X1 \\ X2 \\ X3 \\ X4 \\ X5 \\ X6 \\ X7 \\ X8 \\ X9 \\ X10 \end{pmatrix} + \begin{pmatrix} V1 \\ V2 \\ V3 \\ V4 \\ V5 \\ V6 \\ V7 \\ V8 \\ V9 \\ V10 \end{pmatrix} \quad (34)$$

where

$$\begin{aligned} H51 &= \cos(\Psi) * \tan(\sigma) \\ H61 &= \sin(\Psi) * \tan(\sigma) \end{aligned} \quad (35)$$

$\Psi$  = bearing to subpoint  
 $\sigma$  = maximum elevation angle

as seen in equation 19 and derived in reference (8). The remaining four H components (H55, H56, H65 and H66) are related to the H matrix described briefly in section 3.4.1 (and also derived in reference (8)) above by a simple transformation:

$$\begin{pmatrix} H55 & H56 \\ H65 & H66 \end{pmatrix} = \begin{pmatrix} h11 & h12 \\ h21 & h22 \end{pmatrix} * \begin{pmatrix} -S\sin\theta & S\cos\theta \\ S\cos\theta & S\sin\theta \end{pmatrix} \quad (36)$$

where

S = vehicle speed  
 $\theta$  = vehicle heading

The measurement noise vector V is defined as follows:

$$\begin{pmatrix} V1 \\ V2 \\ V3 \\ V4 \\ V5 \\ V6 \\ V7 \\ V8 \\ V9 \\ V10 \end{pmatrix} = \begin{pmatrix} \text{non-markov (map error - baroaltimeter error)} \\ \text{non-markov (map error - GPS height error)} \\ \text{non-markov (magnetic heading error - gyro error)} \\ \text{non-markov gyro drift rate} \\ \text{static Transit latitude error (in metres)} \\ \text{static Transit longitude error (in metres)} \\ \text{GPS North error (in metres)} \\ \text{GPS East error (in metres)} \\ \text{GPS North velocity error (metres/sec.)} \\ \text{GPS East velocity error (metres/sec.)} \end{pmatrix} \quad (37)$$

and these are assumed to be uncorrelated white noise processes. Measurement noise V5 and V6 are due to the static Transit position fix errors described above in section 3.4.1. The covariance matrix of this noise vector is:

$$R = E\{VV^T\} = \begin{pmatrix} R1 & & & & & & & & & \\ & R2 & & & & & & & & \\ & & R3 & & & & & & & \\ & & & R4 & & & & & & \\ & & & & R5 & & & & & \\ & & & & & R6 & & & & \\ & & & & & & R7 & & & \\ & & & & & & & R8 & & \\ & & & & & & & & R9 & \\ & & & & & & & & & R10 \end{pmatrix} \quad (38)$$

where the numerical values of  $R_i$   $i = 1,8$  are given in Appendix D. These are all constants except for  $R2$ ,  $R3$ ,  $R7$  and  $R8$ .

To estimate the magnetic heading noise covariance  $R_3$  it seems reasonable to assume that its static component is caused by a constant level of noise in the geomagnetic field components. The resulting magnetic heading noise is therefore inversely proportional to the horizontal magnetic field strength, as seen in equation (6) of section 3.2.1 above. Of course a heading noise level of greater than  $\pi$  radians (180 degrees) is physically meaningless, so it is logical to express the static heading noise level (square root covariance in radians) in the form:

$$R_s = \frac{F \cdot R}{(H + F \cdot R / \pi) \cdot \sqrt{N}} \quad (39)$$

where  $H$  is the local horizontal field strength in Gammas,  $F$  is the low latitude field strength in gammas (about 60,000),  $R$  is the low latitude magnetic heading noise level in radians and  $N$  is the number of samples averaged by the prefilter. The  $1/\sqrt{N}$  reduction in noise is due to the prefilter averaging, assuming that the measurement noise is independent, and less than  $\pi$ . Equation (39) will have the correct asymptotic values and approximately the correct  $H$  dependence. The  $R_3$  value shown in Appendix D corresponds to a low latitude magnetic noise  $F \cdot R$  of about 140 gammas and a prefilter level of  $N=60$ , resulting in a low latitude magnetic heading noise  $R$  of about .0025 radians (.15 degrees). Of course at higher latitudes this increases considerably, for example at Resolute (75 degrees latitude -261 degrees longitude)  $H$  is about 522 gammas, resulting in a magnetic heading noise of about .03 radians (1.8 deg.).

In addition to the stationary noise, of magnitude given by equation (39), there is the dynamically induced gimbal error, as described in section 3.2.1. This error depends on the attitude and acceleration of the flux valve gimbals (see equations (7) and (8)); information that is not directly available to the PLANS system. Under normal conditions this acceleration, pitch and roll are due to vehicle vibration and response to the rough driving surface. In other words they are random and of fairly high frequency. It is reasonable to assume that their amplitude is proportional to the vehicles velocity. This dynamic error is therefore modelled as white noise with amplitude (in radians):

$$R_d = \frac{U \cdot S}{H \cdot \sqrt{N}} \quad (40)$$

where  $S$  is the speed,  $H$  is the horizontal field strength,  $N$  is the number of samples averaged by the prefilter and  $U$  is an experimentally determined constant. (Compare to equation (7) of section 3.2.1). The measurement covariance is therefore the sum of the squares of the static and dynamic factors

$$R3 = R_s^2 + R_d^2 \quad (41)$$

The GPS vertical, north and east noise R2, R7 and R8 are modeled simply as constants times the geometric dilution of precision. The MX1107 provides these vertical, north and east dilutions of precision, which are scaled using the constants given in appendix D.

## 6.5 SPECIAL MEASURES

Special measures had to be taken to handle certain difficulties that are expected to arise. One such difficulty will arise if it is necessary to start the system in directional gyro mode without an adequate estimate of the initial heading. Because of this possibility it was necessary to implement a "heading adjustment" parameter, to be added to the directional gyro measurements before they are passed to the navigation filter. The value of this parameter will be initially determined by using the magnetic flux measurement. This value will then be refined at an hourly rate by the Kalman filter itself, as a result of another special measure described below.

This other special measure is necessary whenever directional gyro mode is used for any substantial length of time (10 hours or so). This is because the growing directional gyro heading error will introduce serious nonlinearities into the filter equations. For example the linearized state transition equation (25, 26) carries the implicit assumption that X5 (the gyro heading error) is small. We can ensure that this is the case by in effect "resetting" the directional gyro, every hour. At the same time it is necessary to set the value of X5 in the filter to zero to reflect the corrected gyro. This feature has the added benefit of correcting for any initialization error.

There are various other special functions such as a routine that monitors the Arma Brown gyrocompass output while it is settling, to determine when the settling process has been completed and the gyro's mode can be switched from "settle" to "run".

## 7.0 SIMULATION RESULTS

Throughout the PLANS development activity at DREO, extensive simulations have been performed for three important reasons:

- 1 - system design testing and evaluation
- 2 - algorithm and software testing and evaluation
- 3 - system performance prediction

Extensive Monte-Carlo simulations were performed, first on a PDP 11/34 mini-computer and later on a VAX 780. These simulations predict the PLANS performance under conditions that could not be obtained in the Ottawa area. For example we can simulate high latitude conditions and very long excursions. The simulation runs are also very useful for comparing the performance of many different algorithm designs under identical conditions. Of course simulations are also very fast and cost effective.

A full account of the simulation results will be given in a separate report. A very brief summary of some of the basic simulation results to date is given below. Since there are two different modes of gyro operation, with different performance expectations, we will describe them separately. The primary aim here was to determine whether or not the Kalman filter could correct the velocity errors (especially the heading error) by using the dynamic Transit position fixes.

Simulations were performed using the full PLANS software package, along with specially created measurement generation routines. Monte Carlo and Covariance Analysis techniques were employed to predict the PLANS system performance. For the simulations described below, the "vehicle" started at the initial position 65 degrees north latitude and 100 degrees west longitude, and headed northeast at 10 metres per second. Each Monte Carlo set consisted of 20 simulated runs of 24 hours duration each. In each of the 20 runs of a given set the deterministic errors were exactly the same and the random errors had the same statistical properties (root mean squared values and correlation times) but different actual values. The results of each set were combined to produce one representational run.

## 7.1 GYROCOMPASS MODE

Assuming that the gyro is in gyrocompass mode, then the heading error is bounded to less than a few degrees. The dead reckoning position error will nevertheless increase in time indefinitely, however the Transit errors will be bounded because they depend on the velocity input error. Figure 17 shows the radial position error of the PLANS system over the 24 hour simulation, starting at 65 deg. latitude, -100 deg. longitude, and heading north east with a constant speed of 10 m/s.

As in all of the simulation plots to follow, each point is actually the root-mean-square of 20 points; one from each simulation run. (This is the basis of Monte Carlo simulation, and produces a smoother, more statistically significant plot.) The dashed curve in Figure 17 is the Kalman filter's estimate of its radial position accuracy from the covariance matrix representing the 95% probability level (about 2 sigma).

Figures 18 and 19 show the corresponding radial position errors for the Transit system and the dead reckoning system. It should be mentioned that the "Transit position" was dead-reckoned between position fixes by using the filtered (i.e. PLANS) estimate of velocity, rather than the gyro/odometer measurements, which accounts for the accuracy of this "Transit position". Figure 20 shows the PLANS heading error (solid curve) and the filter's 68% (one sigma) error estimate (dashed). The following overall position accuracy of each of these systems is found by taking the rms of each of these curves over the 24 hours:

PLANS RMS POSITION ERROR	241 metres
TRANSIT RMS POSITION ERROR	248 metres
DR RMS POSITION ERROR	3,973 metres
PLANS RMS HEADING ERROR	.58 degrees
GYROCOMPASS RMS HEADING ERROR	1.0 degrees
FLUX VALVE RMS HEADING ERROR	2.1 degrees

The same simulations were repeated at a higher latitude, in the vicinity of the geomagnetic pole, with a different speed profile. The speed started at zero and increased to 10 m/s over the first two hours, decreased to zero over the next two hours and stayed at zero for four hours. This eight hour sequence was repeated three times, so that the vehicle was stationary for four out of every eight hours. This speed profile is primarily to show the effect of the gyro drift rate measurement when in directional gyro mode, and is used here so that comparison can be made to this gyrocompass mode simulation. The results are as follows:

PLANS RMS POSITION ERROR	586 metres
TRANSIT RMS POSITION ERROR	590 metres
DR RMS POSITION ERROR	10,518 metres

PLANS RMS HEADING ERROR	1.97 degrees
GYROCOMPASS RMS HEADING ERROR	3.7 degrees
FLUX VALVE RMS HEADING ERROR	10.7 degrees

## 7.2 DIRECTIONAL GYRO MODE

The same simulations were repeated with the gyro in directional gyro mode, in which case the heading error would increase without bound resulting in a much faster growth in the DR position error and, more importantly, a potential for unbounded growth in the Transit position error (if the Kalman filter can not adequately estimate and remove the gyro error). The results starting at 65 degrees latitude, with constant speed, are illustrated in Figure 21, 22, 23 and 24, where it can be seen that the filter performed very well. The corresponding numerical results are:

PLANS RMS POSITION ERROR	282 metres
TRANSIT RMS POSITION ERROR	303 metres
DR RMS POSITION ERROR	21,426 metres

PLANS RMS HEADING ERROR	.67 degrees
DIRECTIONAL GYRO RMS HEADING ERROR	4.5 degrees
FLUX VALVE RMS HEADING ERROR	2.1 degrees

The same simulations were repeated with the gyro in directional gyro mode, with the periodic velocity profile at the higher latitude, near the geomagnetic pole. This is to show the effect of the gyro drift rate measurement. The results are:

PLANS RMS POSITION ERROR	350 metres
TRANSIT RMS POSITION ERROR	326 metres
DR RMS POSITION ERROR	10,640 metres

PLANS RMS HEADING ERROR	.96 degrees
DIRECTIONAL GYRO RMS HEADING ERROR	6.4 degrees
FLUX VALVE RMS HEADING ERROR	10.7 degrees

It should be again clarified that this "Transit" position accuracy is due to the fact that it uses the PLANS filter velocity estimate between fixes.

Figure 17. SIMULATION PLANS POSITION ERROR AND COVARIANCE

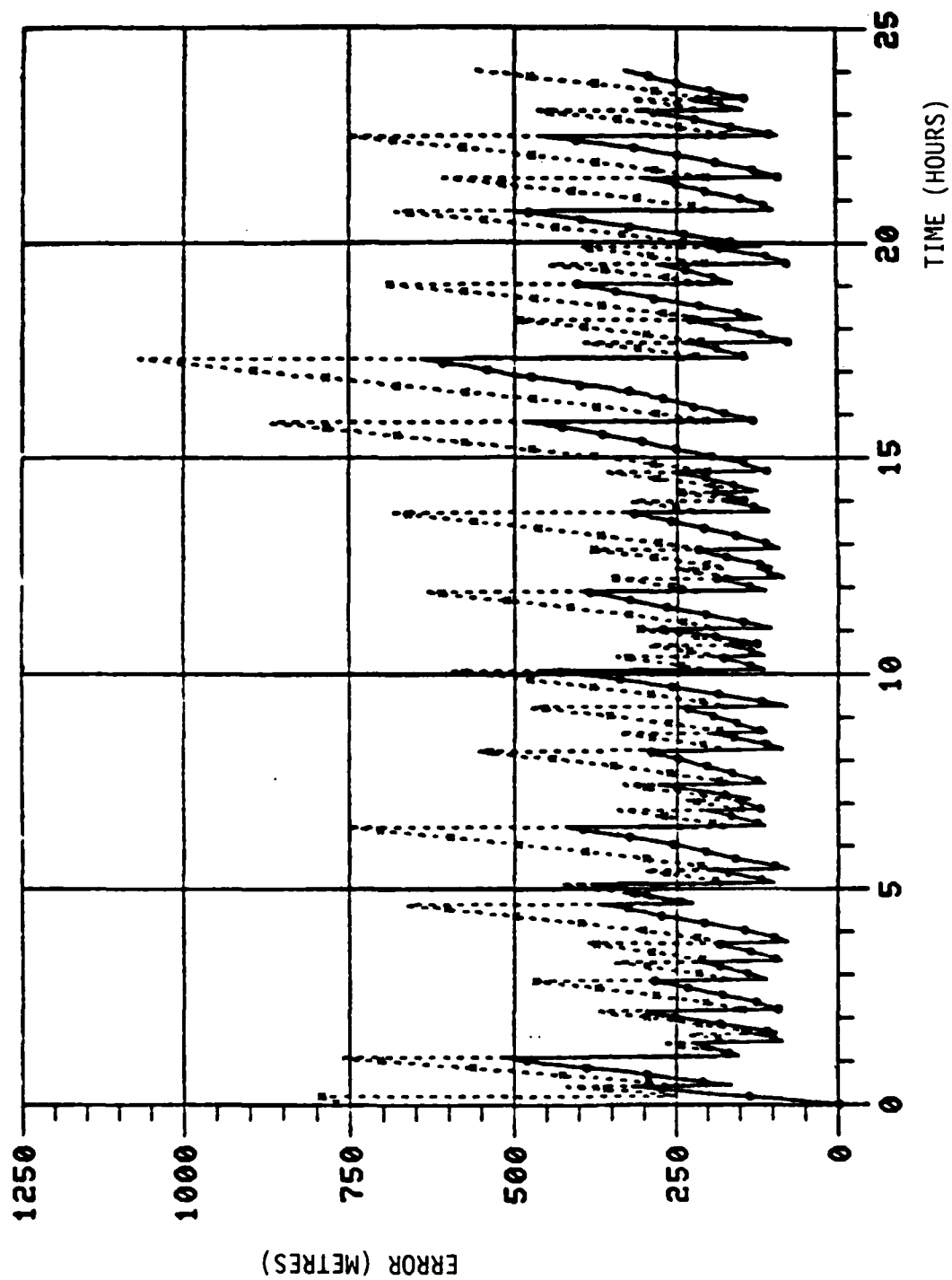


Figure 18. SIMULATION TRANSIT POSITION ERROR

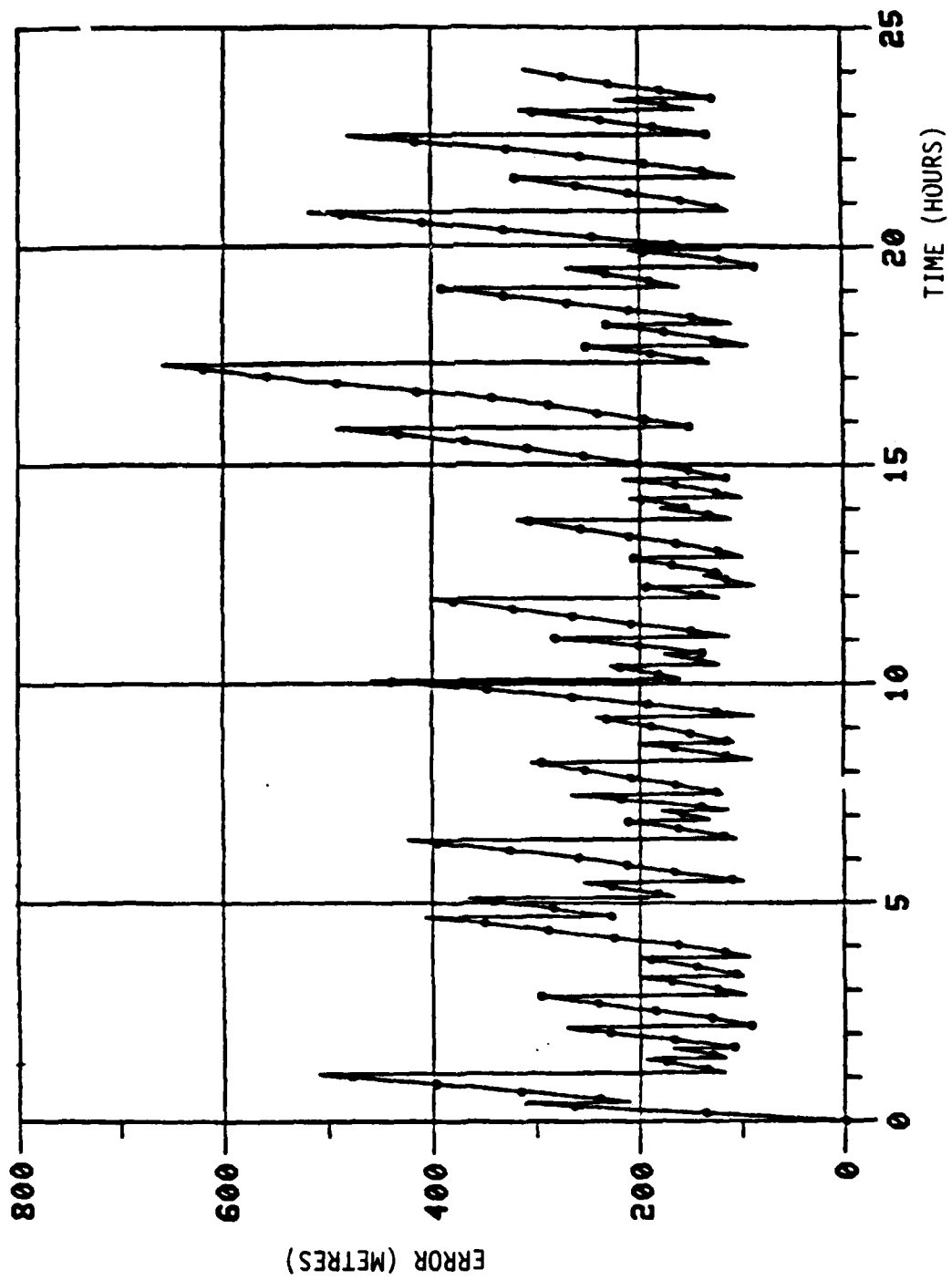


Figure 19. SIMULATION DEAD-RECKONING POSITION ERROR

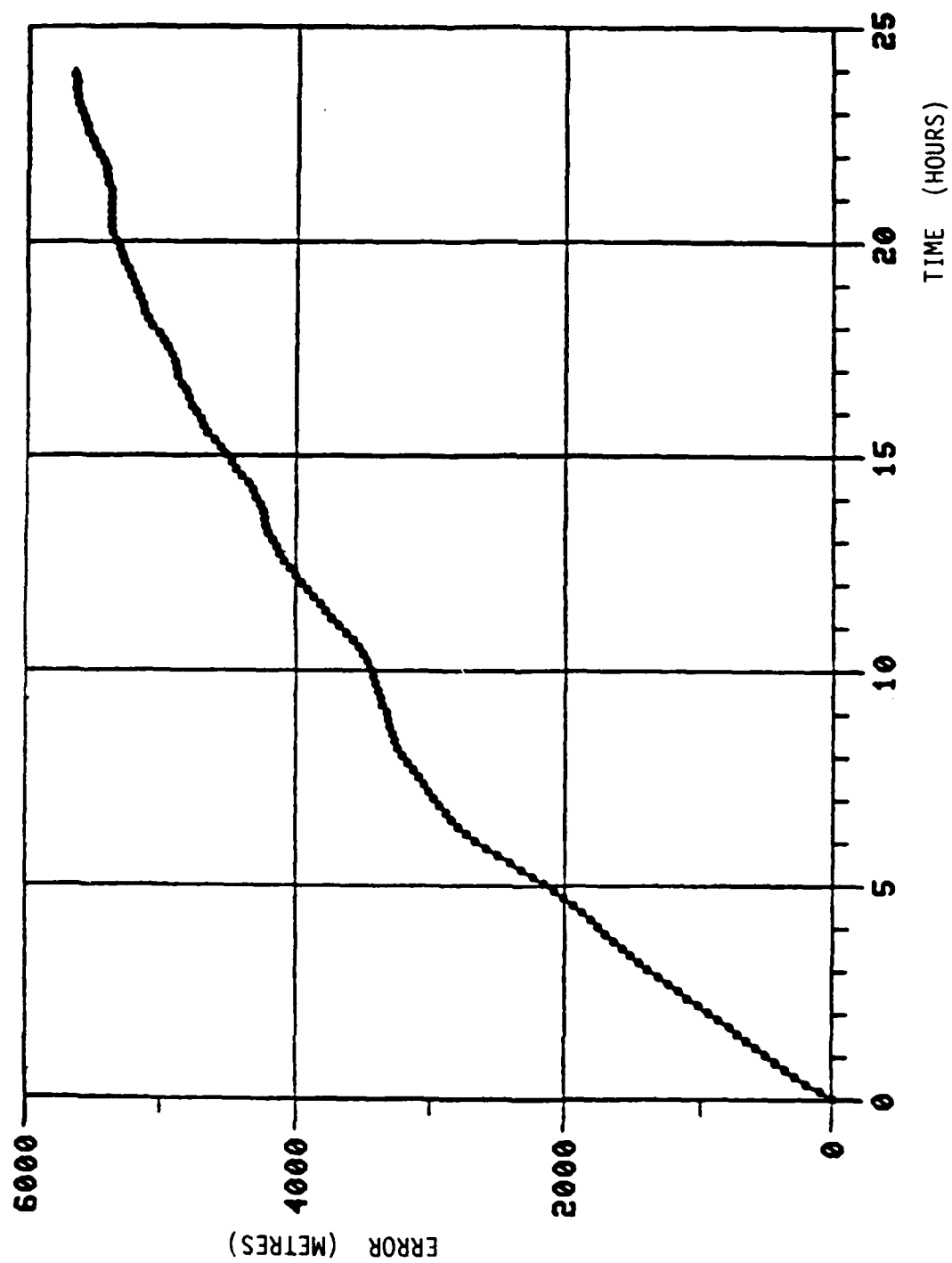


Figure 20. SIMULATION PLANS HEADING ERROR AND COVARIANCE

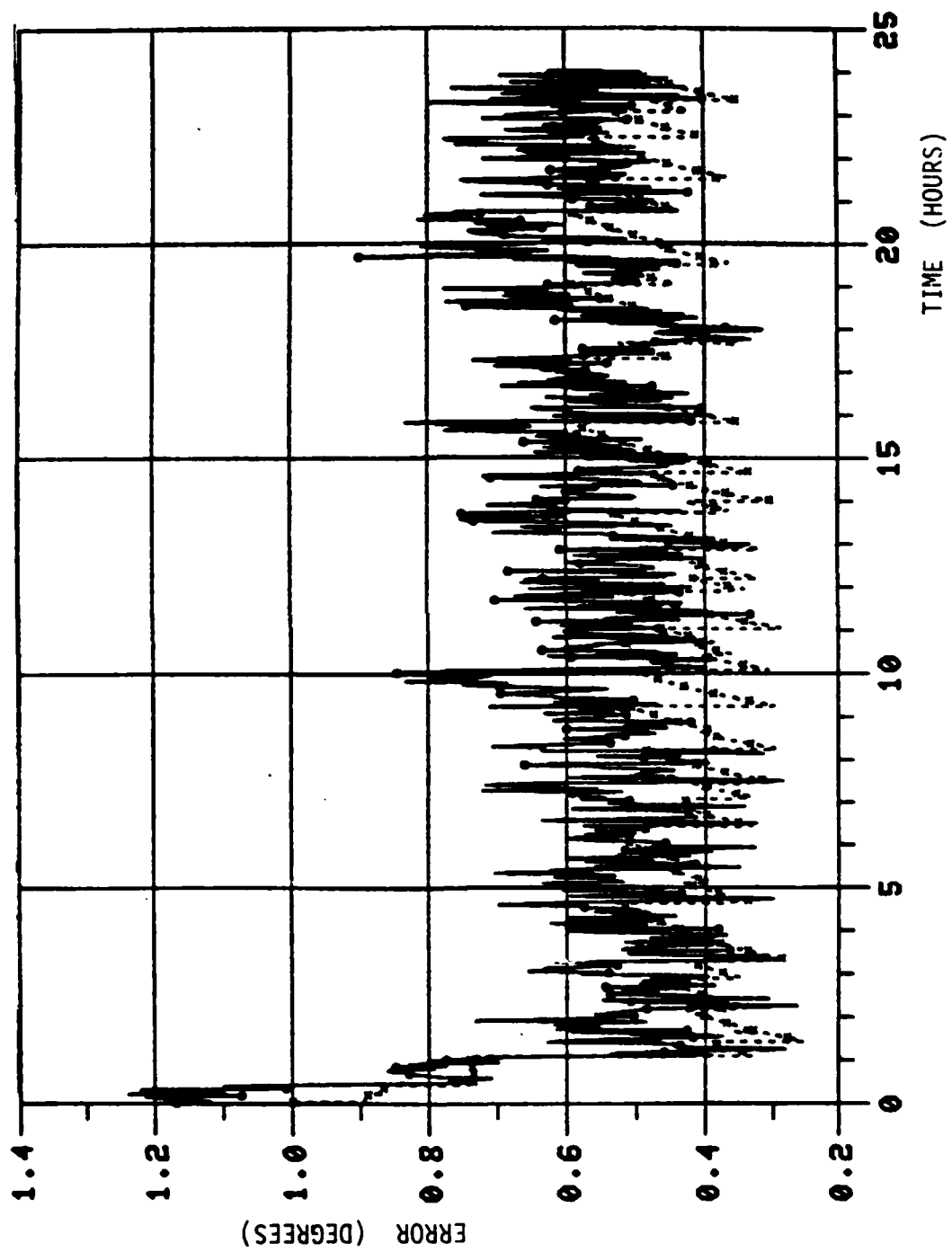


Figure 21. SIMULATION PLANS POSITION ERROR AND COVARIANCE

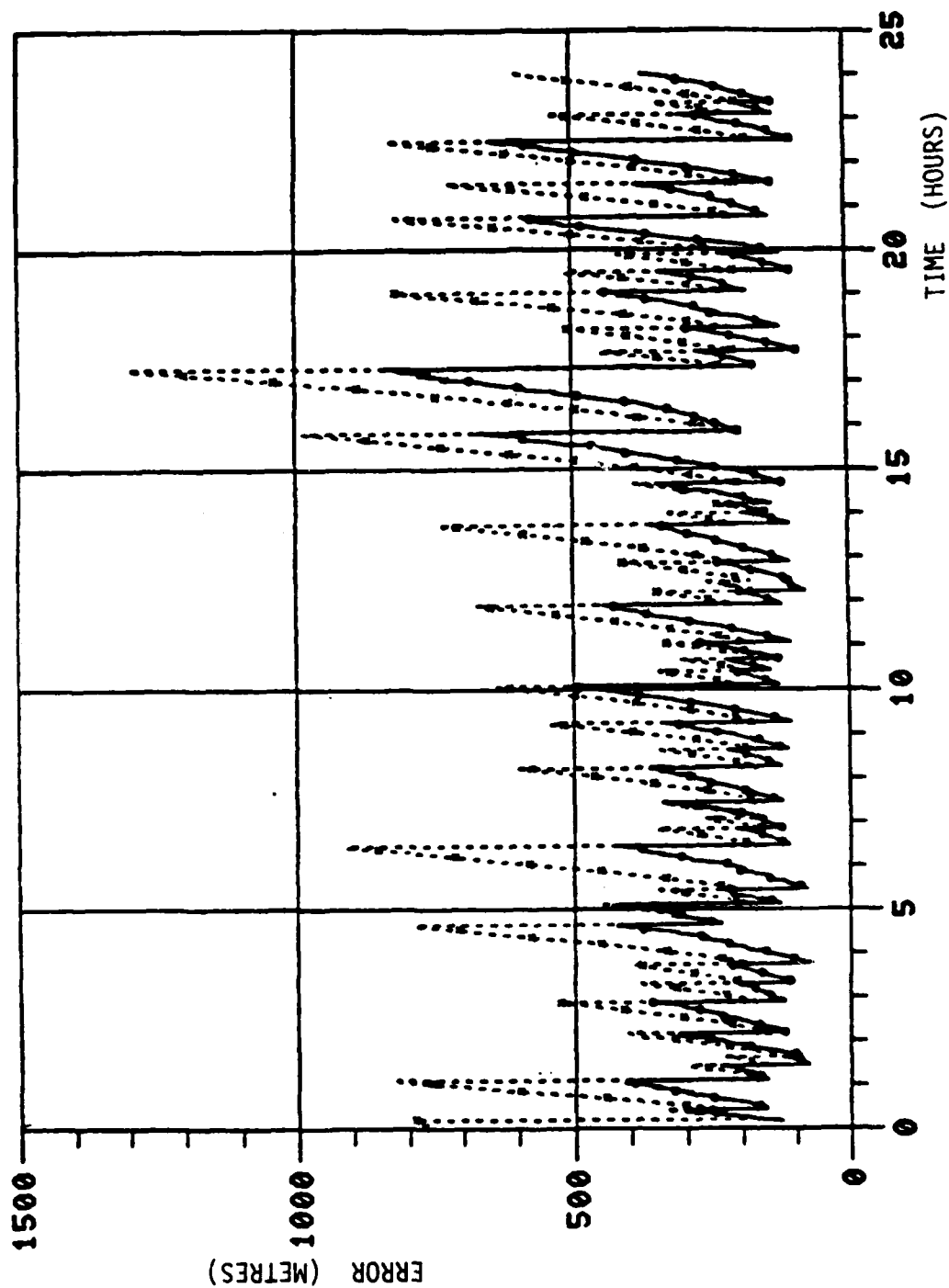


Figure 22. SIMULATION TRANSIT POSITION ERROR

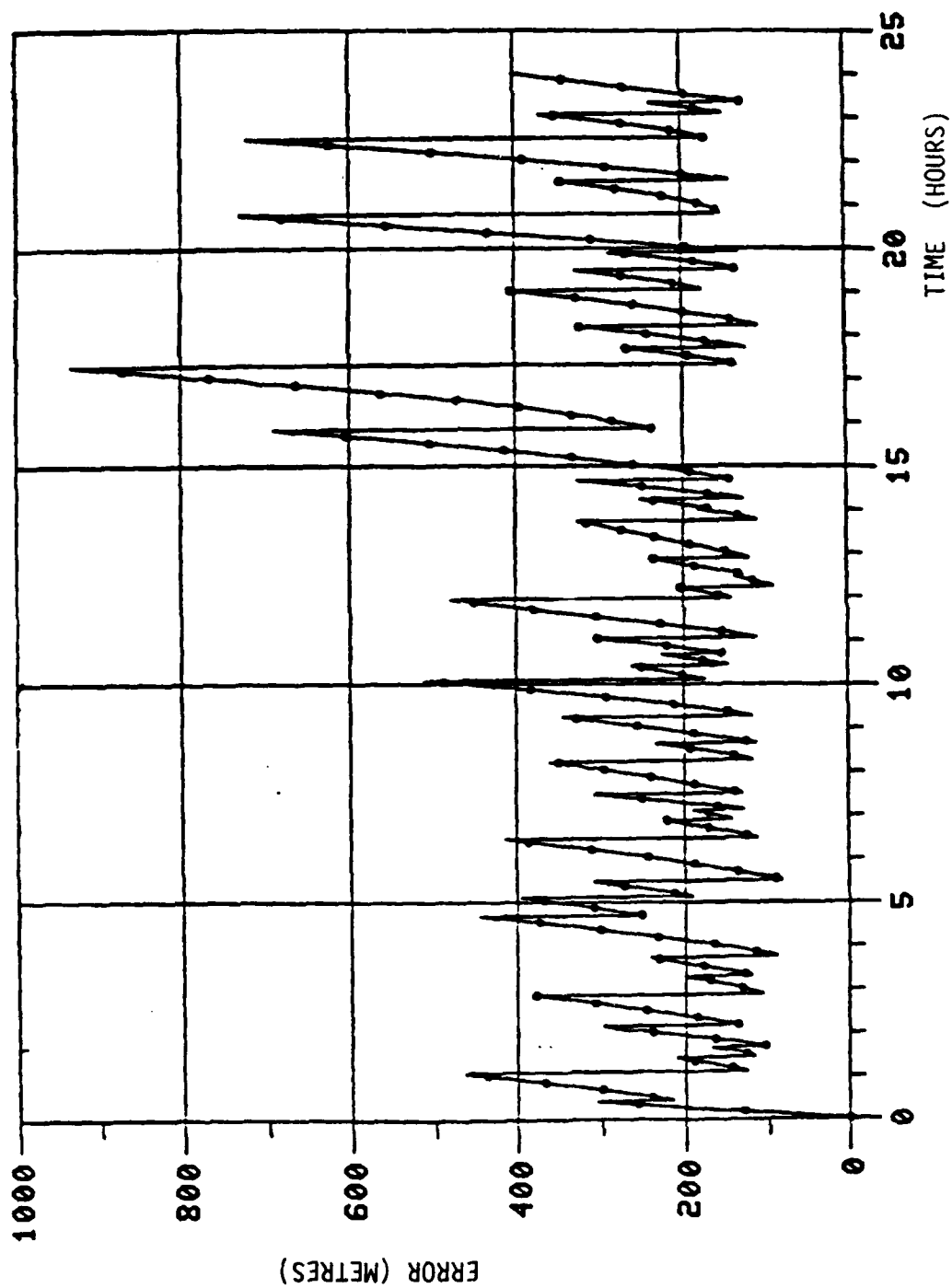


Figure 23. SIMULATION DEAD-RECKONING POSITION ERROR

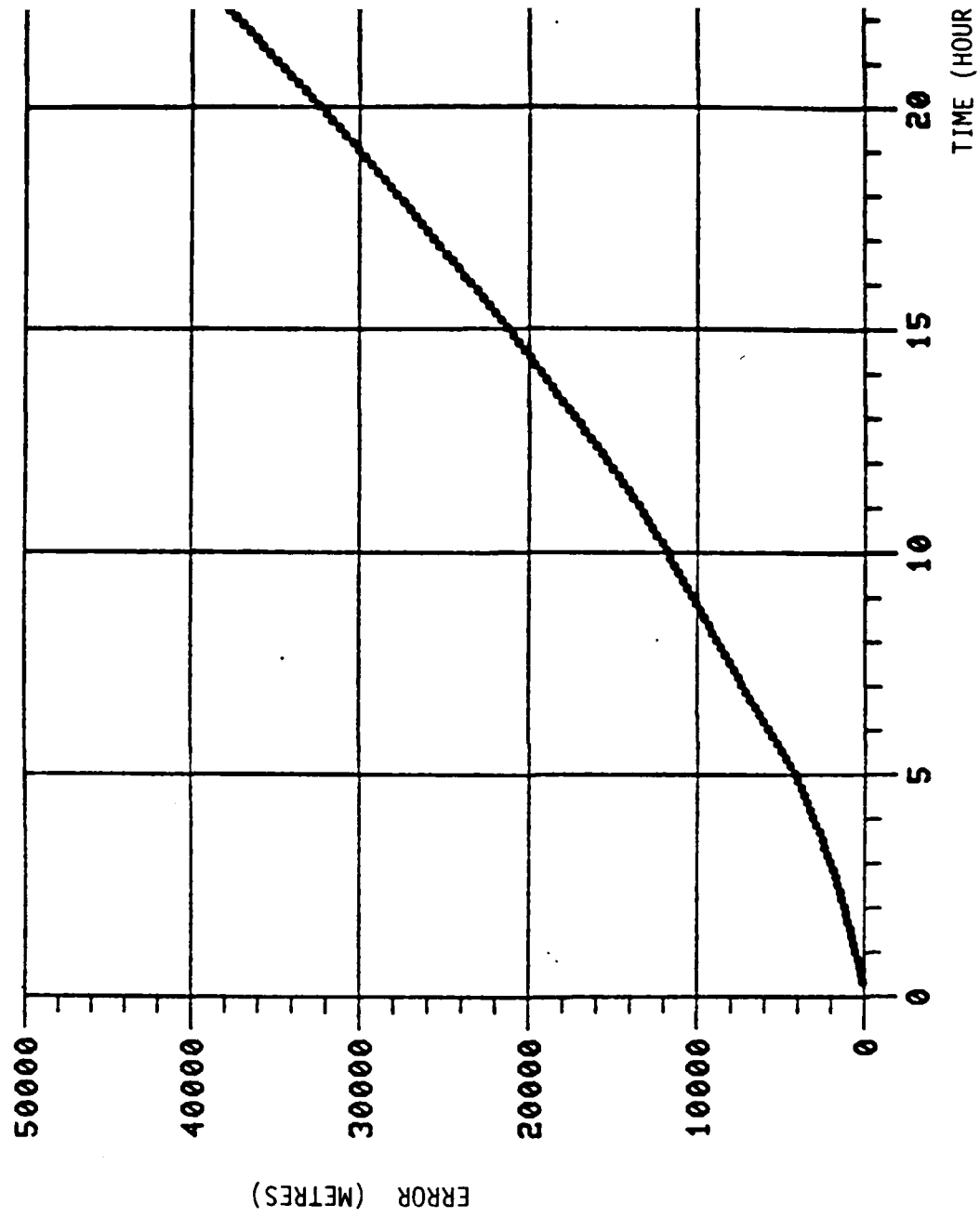
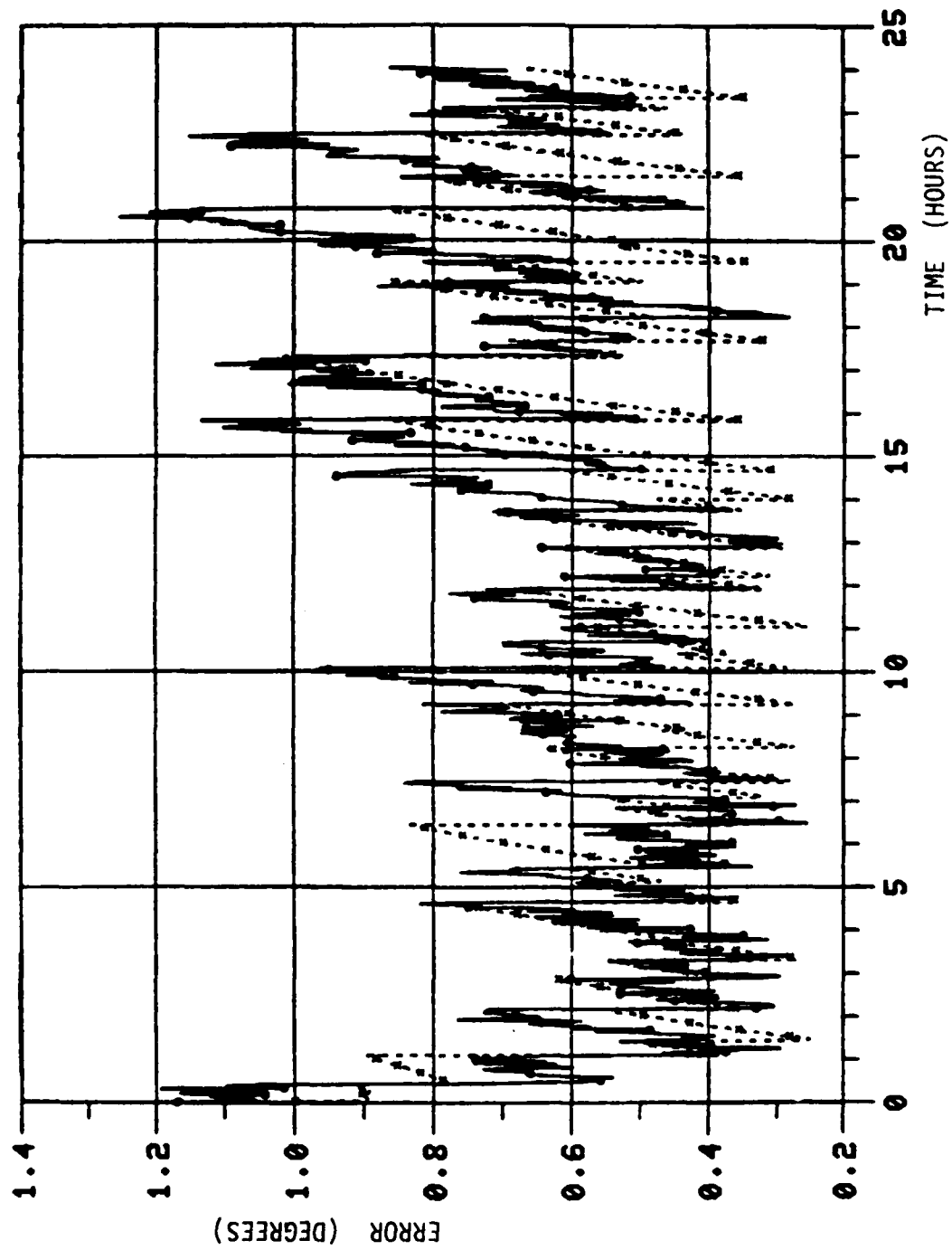


Figure 24. SIMULATION PLANS HEADING ERROR AND COVARIANCE



## 8.0 SUMMARY

A complete optimally integrated navigation system for arctic land navigation has been designed and constructed at DREO. All necessary sensors, processors and displays have been identified, purchased, tested and interfaced to:

- 1 - Arma Brown MK V (Mod 4) dual mode gyro
- 2 - Magnovox MX1107 dual channel Transit/GPS receiver
- 3 - Masstech TR10 pickoff for the APC odometer
- 4 - Marinex Compass Sensor Unit Type 900111 (fluxgate)
- 5 - Setra Systems High Output Pressure Transducer model 205-2
- 6 - Motorola 68000 microprocessor
- 7 - Data Images custom LCD displays
- 8 - Lear Siegler VRU (Vertical Reference Unit)
- 9 - Lear Siegler DMU (Distance Measurement Unit)

The necessary algorithms and data bases have been acquired or developed to obtain the most accurate possible navigation information from these sensor measurements, including a full geomagnetic field model algorithm and a digital arctic elevation map data base. A detailed functional relationship has been derived which explicitly describes the dynamic Transit position fix errors in such a way as to allow heading information to be extracted from the Transit position fixes.

An eight state extended Kalman filter has been designed and implemented to optimally integrate all sensor information. Extensive simulations have been conducted to test the PLANS system design. The results of these simulations are very positive and shall soon be reported in more detail. Local field trials have been conducted to test the real-time PLANS software, the sensors and the sensor interfaces, and to refine the error models required in the Kalman filter design. Figures 25 and 26 show some of the PLANS equipment during these local trials.

More trials, of longer duration, were necessary to obtain reliable performance figures. Therefore a week long field trial was conducted at Canadian Forces Base Petawawa, on November 25-29, 1985. The course chosen was the 55 km. long perimeter road, a closed circuit with frequent changes in heading and elevation. The surface condition was hard packed snow, causing noticeable track slippage, and the driving speed was quite high, up to 75 km/hr. The results of this trial are in general agreement with the previous simulation predictions. When the Arma Brown gyro was

used, the PLANS RMS position error was less than 250 m on 4 out of the 5 circuits that have been analysed. This is less than .5% of distance travelled and is somewhat better than would be expected in arctic conditions. Figures 27 and 28 show the general state of the equipment installed for this trial.

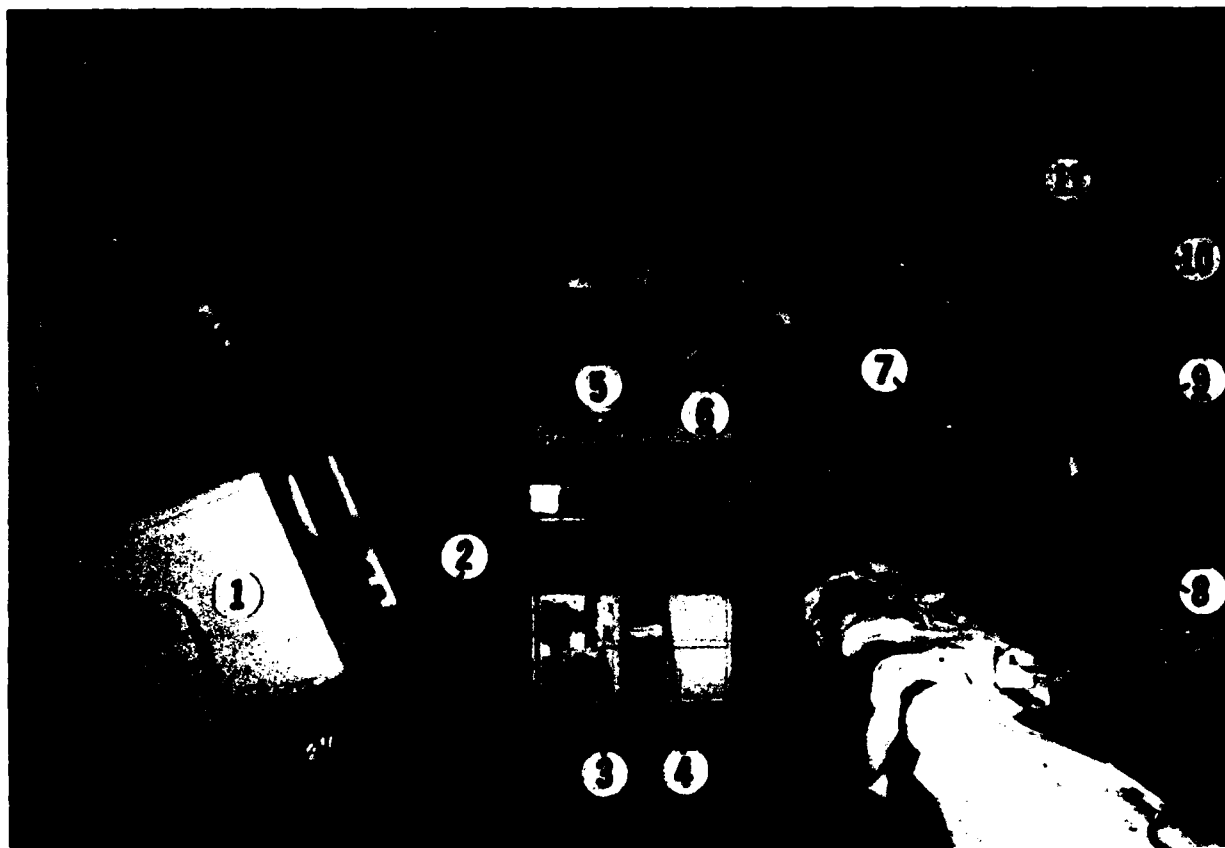
As of March 1986, the search is continuing for a better fluxgate sensor, a better gyrocompass (or equivalent) as well as a more accurate and/or extensive terrain elevation data base. A DOWTY Model TAM 7, 3-axis strapdown hybrid magnetometer looked promising and was ordered, but it is not yet a production item, and its specifications have already been significantly revised since the order was placed. It may consequently prove to be unacceptable for environmental reasons (mostly temperature). The Lear Siegler gyro, which is also not yet in production, showed initial promise as a replacement for the Arma Brown, but has also demonstrated some serious limitations. These are now being addressed by the manufacturer with our assistance.

Figure 25. EXTERNAL VIEW OF 1984 INSTALLATION



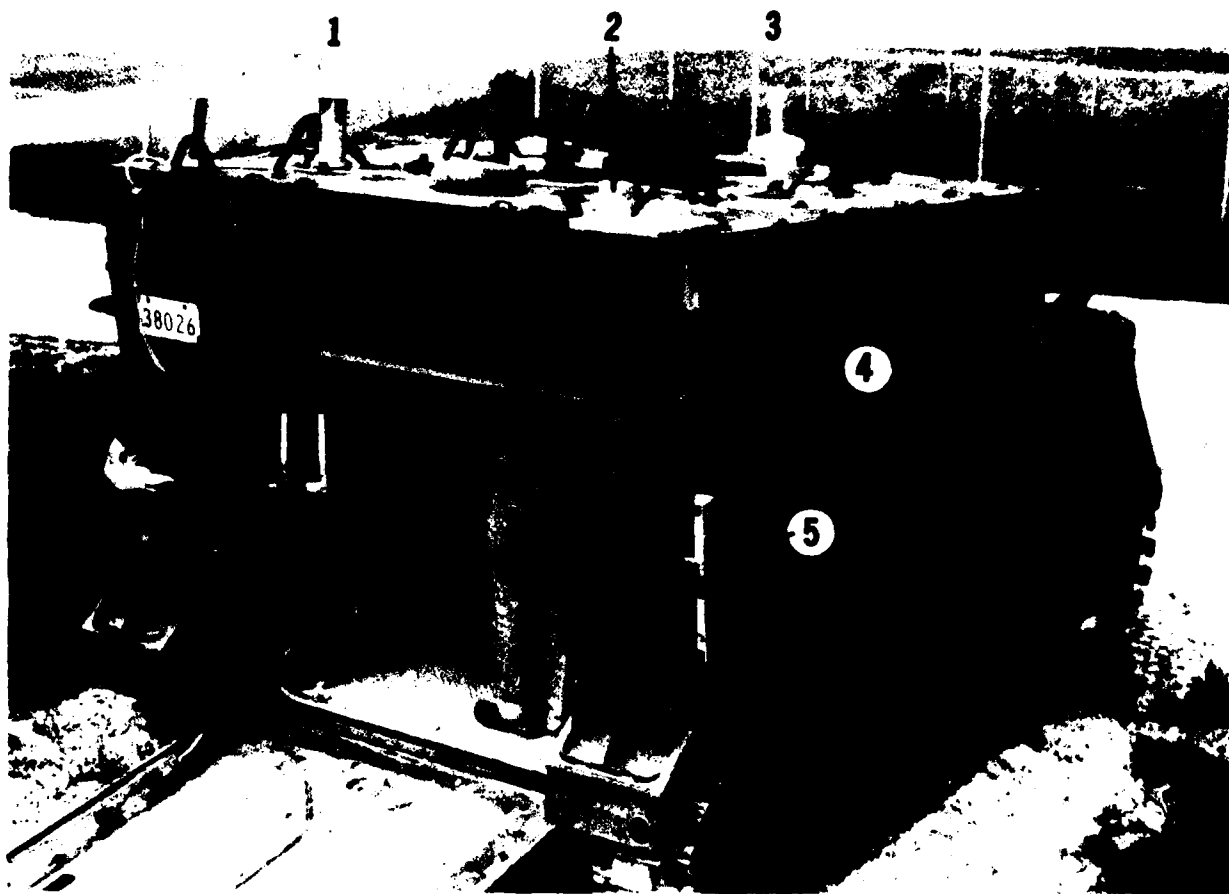
1. M113 Armoured Personnel Carrier
2. Antenna for MX1105 Transit Receiver
3. Infra Red Sensor for Test Equipment

Figure 26. INTERNAL VIEW OF 1984 INSTALLATION



1. MX1105 Transit Receiver
2. Printer
3. Motorola 68000 Microprocessor
4. Sealed Disk and Floppy Disk Drives
5. Video Display
6. LSI 11/23 Microcomputer
7. Inverter for Gyrocompass
8. Control Unit for Gyrocompass
9. Arma Brown Dual Mode Gyrocompass
10. Baroaltimeter
11. Inclimeters

Figure 27. EXTERNAL VIEW OF 1986 INSTALLATION



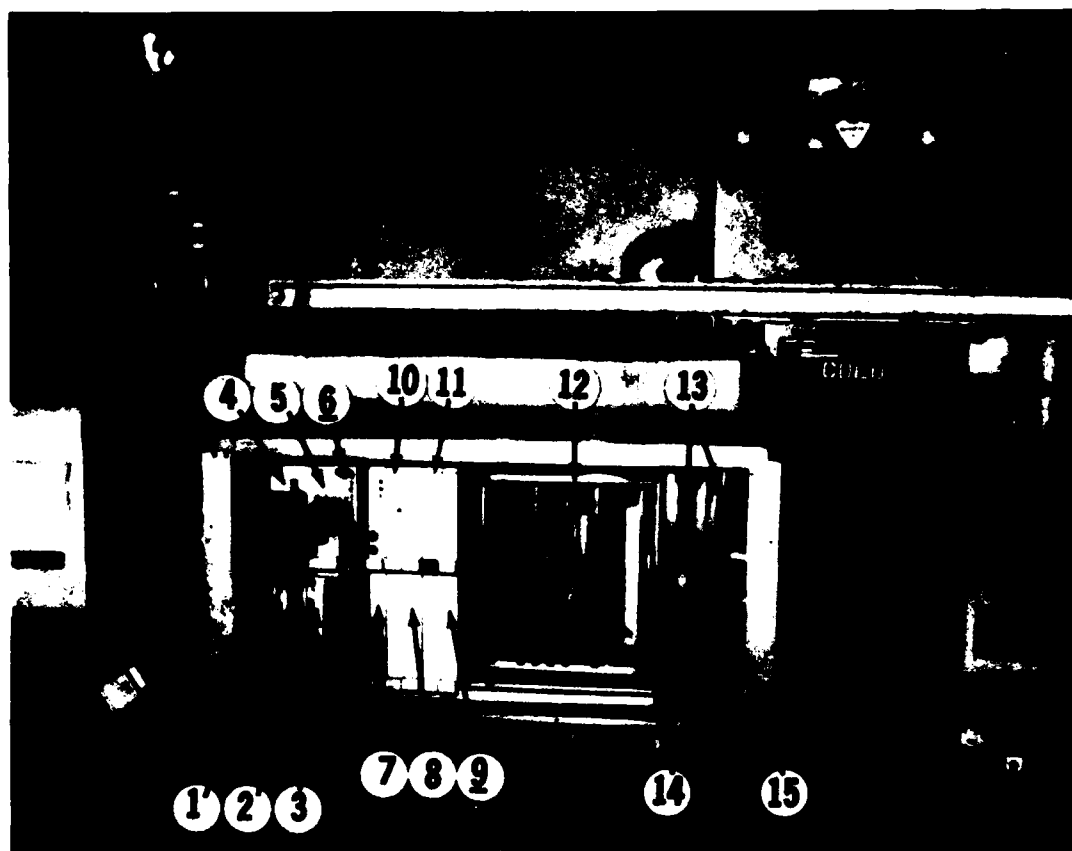
1. Dual Channel Transit Antenna
2. Marinex Magnetic Compass Unit (gimballed)
3. GPS Antenna
4. M577 Command Vehicle
5. Infra Red Sensor (test equipment)

Figure 28. INTERNAL VIEW OF 1986 INSTALLATION



1. MX1107 Monitor (test equipment)
2. Video Display (temporary PLANS Main Display)
3. Terminal for Data Recording System (test equipment)
4. Remote PLANS Display
5. Arma Brown Gyrocompass (test Equipment)
6. Inverter for Arma Brown Gyrocompass (test equipment)
7. PLANS Central Unit (see Figure 29 for contents)
8. PLANS Main Display (not installed here)
9. PLANS Keypad
10. Lear Siegler Vertical Reference Unit

Figure 29. PLANS Central Unit, 1986



1. General Purpose Interface Card (GPI)
2. Quad Serial Port (QSP)
3. Analog Board
4. Synchro to Digital Converter (for Arma Brown test equipment)
5. Motorola Dual RS232 (for test equipment)
6. Analog to Digital Converter (8 differential channels)
7. Motorola 68000 Processor
8. EPROM
9. Extra EPROM
10. RAM
11. Floating Point Processor
12. MX1107 Electronics Chassis
13. MX1107 Oscillators
14. Power Supplies
15. Baroaltimeter (Setra 205-2 pressure transducer)

## REFERENCES

- (1) Task DLAEEM 103, "Investigation of a Primary Land Arctic Navigation System"
- (2) DiFilippo, D., "Primary Land Arctic Navigation System, Preliminary Results of Recommendation Study", DREO Task DLAEEM 103 Report, July 1982.
- (3) Task DLAEEM 108, "Development of a Primary Land Arctic Navigation System (PLANS)", Nov. 1982.
- (4) Gupta, R.R., Donnelly, S.F., Creamer, P.M., and Sayer, S., "Omega Signal Coverage Prediction Diagrams for 10.2 KHz", Document prepared by the Analytic Sciences Corporation for the U.S. Department of Transportation, U.S. Coast Guard, ONSOD, October 1980 (final report).
- (5) Malin, S.R.C., and Barraclough, D.R., Computers and Geosciences, Vol. 7 (1981), No. 4, pp. 401-405.
- (6) Whitham, K., Loomer, E.I., and Niblett, E.R., "The Latitudinal Distribution of Magnetic Activity in Canada", J. of Geophysical Research, Vol 65, No. 12, December 1960.
- (7) Ayers, H., "Azimuth Determination Using Transit Satellite System", Technical report prepared by JMR Instruments Canada Ltd. for the Defence Research Establishment Ottawa, July 1983.
- (8) McMillan, J.C., unpublished notes.
- (9) Vanicek, P., and Krakiwsky, E.J., "Geodesy: The Concepts". North-Holland Publishing Co., 1982.
- (10) Paquet, F., "Speed Sensor Calibration on an Armoured Personnel Carrier" DREO Technical Memorandum, Tech # 9/84, February 1984.
- (11) Anderson, J.D. Jr., "Introduction to Flight", McGraw-Hill, 1978, p. 59.
- (12) Kayton, M., and Fried, W.R., editors, "Avionics Navigation Systems", John Wiley and Sons, Inc. Toronto, 1960.
- (13) Veale, B., D. Met Oc, private communication, 1984.
- (14) Stansell, T.A., "Transit, The Navy Navigation Satellite System", Navigation, Vol. 18, No. 1, Spring 1973.
- (15) Janiczek, P.M., editor, "Global Positioning System, Papers published in Navigation", reprinted by the Institute of Navigation, Washington, D.C., 1980.

REFERENCES

- (16) Gelb, A., Editor, "Applied Optimal Estimation", The Analytic Sciences Corporation, The M.I.T. Press, Cambridge, Massachusetts, 1974.
- (17) Dion, M., "Development of a Multiple Port Serial Interface Module for PLANS", DREO Technical Note No. 85/28, 1985.
- (18) Dion, M., "Development of a General Purpose Interface Module for PLANS", DREO Technical Note No. 86/ , 1986.

UNCLASSIFIED

Security Classification

DOCUMENT CONTROL DATA - R & D		
(Security classification of title, body of abstract and indexing annotation must be entered when the overall document is classified.)		
1. ORIGINATING ACTIVITY Defence Research Establishment Ottawa Ottawa, Ontario K1A 0Z4		2a. DOCUMENT SECURITY CLASSIFICATION UNCLASSIFIED
		2b. GROUP
3. DOCUMENT TITLE Design of an Optimally Integrated Primary Land Arctic Navigation System (PLANS), Volume I: System Design (U)		
4. DESCRIPTIVE NOTES (Type of report and inclusive dates) DREO Report		
5. AUTHOR(S) (Last name, first name, middle initial)  McMillan, Joseph C.		
6. DOCUMENT DATE	7a. TOTAL NO. OF PAGES 71	7b. NO. OF REFS 18
8a. PROJECT OR GRANT NO  041LJ	9a. ORIGINATOR'S DOCUMENT NUMBER(S)  DREO Report #: 946	
8b. CONTRACT NO	9b. OTHER DOCUMENT NO.(S) (Any other numbers that may be assigned this document)	
10. DISTRIBUTION STATEMENT Unlimited Distribution		
11. SUPPLEMENTARY NOTES		12. SPONSORING ACTIVITY DLAEM 4-2
13. ABSTRACT - UNCLASSIFIED <p>This land navigation system is designed around a dual mode gyrocompass/directional gyro, and the vehicle's odometer, with occasional Transit position fixes. A baroaltimeter is used to provide height above ellipsoid needed by the Transit receiver, and a coarse digital elevation map is used to bound the error in the barometric height. An inexpensive magnetic flux valve is used, in conjunction with a geomagnetic field model, to augment the gyro and provide a rough initial heading. An eight state extended Kalman Filter was designed to process the measurements from these sensors and thus provide an optimal estimate of the vehicles position, velocity and bearing. //</p> <p>Perhaps the most significant new aspect of this design is its ability to correct for the otherwise unbounded heading errors that are typical of directional gyro operation at high latitudes, where gyrocompassing is not possible and near the magnetic pole, where magnetic compasses are useless. In this design a heading correction is automatically performed whenever a Transit position fix is received while the vehicle is underway (about once every hour at high latitudes) This unique capability is due to a detailed deterministic error model, developed at DREO, which relates the error in the velocity fed into the Transit receiver during a satellite pass, to the error in the position fix that this pass yields.</p>		

UNCLASSIFIED

Security Classification

KEY WORDS

Navigation  
Kalman filter  
Integrated System  
Optimal Estimation  
Arctic

INSTRUCTIONS

1. **ORIGINATING ACTIVITY:** Enter the name and address of the organization issuing the document.
- 2a. **DOCUMENT SECURITY CLASSIFICATION:** Enter the overall security classification of the document including special warning terms whenever applicable.
- 2b. **GROUP:** Enter security reclassification group number. The three groups are defined in Appendix 'M' of the DRB Security Regulations.
3. **DOCUMENT TITLE:** Enter the complete document title in all capital letters. Titles in all cases should be unclassified. If a sufficiently descriptive title cannot be selected without classification, show title classification with the usual one-capital-letter abbreviation in parentheses immediately following the title.
4. **DESCRIPTIVE NOTES:** Enter the category of document, e.g. technical report, technical note or technical letter. If appropriate, enter the type of document, e.g. interim, progress, summary, annual or final. Give the inclusive dates when a specific reporting period is covered.
5. **AUTHOR(S):** Enter the name(s) of author(s) as shown on or in the document. Enter last name, first name, middle initial. If military, show rank. The name of the principal author is an absolute minimum requirement.
6. **DOCUMENT DATE:** Enter the date (month, year) of Establishment approval for publication of the document.
- 7a. **TOTAL NUMBER OF PAGES:** The total page count should follow normal pagination procedures, i.e., enter the number of pages containing information.
- 7b. **NUMBER OF REFERENCES:** Enter the total number of references cited in the document.
- 8a. **PROJECT OR GRANT NUMBER:** If appropriate, enter the applicable research and development project or grant number under which the document was written.
- 8b. **CONTRACT NUMBER:** If appropriate, enter the applicable number under which the document was written.
- 9a. **ORIGINATOR'S DOCUMENT NUMBER(S):** Enter the official document number by which the document will be identified and controlled by the originating activity. This number must be unique to this document.
- 9b. **OTHER DOCUMENT NUMBER(S):** If the document has been assigned any other document numbers (either by the originator or by the sponsor), also enter this number(s).
10. **DISTRIBUTION STATEMENT:** Enter any limitations on further dissemination of the document, other than those imposed by security classification, using standard statements such as:
  - (1) "Qualified requesters may obtain copies of this document from their defence documentation center."
  - (2) "Announcement and dissemination of this document is not authorized without prior approval from originating activity."
11. **SUPPLEMENTARY NOTES:** Use for additional explanatory notes.
12. **SPONSORING ACTIVITY:** Enter the name of the departmental project office or laboratory sponsoring the research and development. Include address.
13. **ABSTRACT:** Enter an abstract giving a brief and factual summary of the document, even though it may also appear elsewhere in the body of the document itself. It is highly desirable that the abstract of classified documents be unclassified. Each paragraph of the abstract shall end with an indication of the security classification of the information in the paragraph (unless the document itself is unclassified) represented as (TS), (S), (C), (R), or (U).

The length of the abstract should be limited to 20 single-spaced standard typewritten lines, 7 1/2 inches long
14. **KEY WORDS:** Key words are technically meaningful terms or short phrases that characterize a document and could be helpful in cataloging the document. Key words should be selected so that no security classification is required. Identifiers, such as equipment model designation, trade name, military project code name, geographic location, may be used as key words but will be followed by an indication of technical context.